Ancestral genome reconstruction reveals the history of ecological diversification in *Agrobacterium*.

Florent Lassalle[1,2,3] *, Rémi Planel[2], Simon Penel[2], David Chapulliot[1], Valérie Barbe[4], Audrey Dubost[1], Alexandra Calteau[4,5,6], David Vallenet[4,5,6], Damien Mornico[4,5,6], Thomas Bigot[2], Laurent Guéguen[2], Ludovic Vial[1], Daniel Muller[1], Vincent Daubin[2], Xavier Nesme[1].

[1] *Univ Lyon, CNRS, INRA, VetAgro Sup, UCBL, Ecologie Microbienne, 69622 Villeurbanne, France.*

[2] *Univ Lyon, CNRS, UCBL, Biométrie et Biologie Evolutive, 69622 Villeurbanne, France.*

[3] *Ecole Normale Supérieure de Lyon, 69342 Lyon, France*

[4] *Direction de la Recherche Fondamentale, Commissariat à l'Energie Atomique et aux Energies Alternatives (CEA), Institut de Génomique, Genoscope, 2 rue Gaston Crémieux, Evry F-91057, France.*

[5] *CNRS, UMR 8030, Laboratoire d'Analyse Bioinformatiques pour la Génomique et le Métabolisme , 2 rue Gaston Crémieux, 91057 Evry, France*

[6] *UEVE, Université d'Evry Val d'Essonne, boulevard François Mitterrand, 91025 Evry, France*

** Author for correspondence: Florent Lassalle, MRC Center for Outbreak Analysis and Modelling, Imperial College London, Praed Street, London W2 1NY, +44 207 594 1379, f.lassalle@imperial.ac.uk*

Abstract

Horizontal gene transfer (HGT) is considered a major source of innovation in bacteria, and as such is expected to drive the adaptation to new ecological niches. However, among the many genes acquired through HGT along the diversification history of genomes, only a fraction may have actively contributed to sustained ecological adaptation. Here, we use a phylogenetic approach accounting for the transfer of genes (or groups of genes) to reconstruct the history of genomes in *Agrobacterium* biovar 1, a diverse group of soil and plant-dwelling bacterial species. We identify clade-specific blocks of co-transferred genes encoding coherent biochemical pathways that may have contributed to the evolutionary success of key *Agrobacterium* clades. This pattern of gene co-evolution rejects a neutral model of transfer, in which neighbouring genes would be transferred independently of their function and suggests purifying selection on collectively coded acquired pathways. We argue that these synapomorphic blocks of co-functioning genes which consistently hint at the strong selective role of host plant rhizospheres, have driven the ecological diversification of *Agrobacterium* and define features of ancestral ecological niches.

Keywords: reverse ecology; ancestral genome; HGT; tree reconciliation; co-transferred genes; *Agrobacterium tumefaciens*.

Introduction

Our understanding of the ecology of bacteria is fragmentary. We usually know a subset of the environments from which a species can be sampled, some laboratory conditions in which they can be grown, and sometimes the type of interactions they establish with other organisms. We now also have their genomes, which we believe contain all the information that make their lifestyle possible. However, even if we could describe the molecular function of every base in a genome, it would not necessarily allow us to understand whether this function is significant in its prevalent environment (Doolittle 2013). Another approach consists in recognizing traces of selection for functional adaptation in the histories of genomes. The comparison of genomes reveals a historical signal that can be used to reconstruct genome evolution, their hypothetical ancestral state, and the course of evolutionary events that shaped them in time. Using models of null expectation under neutral evolution, we can discern the events that have been decisive in the adaptive evolution of species. Bacterial genomes are in constant flux, with genes being gained and lost at rates that can exceed the nucleotide substitution rate (Lawrence & Ochman 1997). Recognition of these dynamics led to the definition of the concept of pangenome, the set of all homologous gene families present in a group of related genomes. The pangenome comprises is the sum of core and accessory genomes, which respectively gather the genes that are shared by all genomes in the dataset and those that are found in some genomes but not all. In *E. coli*, for example, the core genome is estimated to have 1,800 gene families, while the accessory genome has more than 80,000 gene families, with two random strains differing typically by a thousand

(Touchon et al. 2009; Land et al. 2015). Accessory genes are regularly gained in a genome by transfer or quickly lost, leaving patterns of presence in genomes that are inconsistent with the strains' phylogeny (Young 2016). For a majority of accessory gene families, this process occurs so rapidly that they are effectively observed in a single genome, caught by the snapshot of genome sequencing, suggesting they have only ephemeral, if any, adaptive value for their bacterial host (Daubin et al. 2003). However, this constant input of genes also allows adaptative accessory genes to settle in genomes, and become part of the core genome of a lineage. Such 'domestication' events in the midst of rapid turnover of genome gene content constitute the most remarkable deviations from a neutral model where all genes are equally likely gained and lost. Clade-specific conservation of a gene is thus suggestive of adaptation to a particular ecological niche (Lassalle et al. 2015).

In a previous study, we explored the diversity of gene repertoires among strains of *Agrobacterium* biovar 1 that contains several bona fide but yet unnamed 'genomic' species G1 to G9 and G13, collectively named '*Agrobacterium tumefaciens* species complex' (*At*) according to the proposal of Costechareyre et al. (Costechareyre et al. 2010). We found that genes specific to the species under focus – G8, for which we proposed the name *A. fabrum* – were in majority clustered in the genome, and that these clusters gathered genes that encoded coherent biological functions (Lassalle et al. 2011). The conservation of co-functioning genes in genomic clusters appears unlikely in the context of frequent gene turnover. This pattern could be a trace of purifying selection acting to retain the gene clusters in their wholeness, because the selected unit is the function collectively encoded by the constituent genes. However, it could also result from a neutral process of gene flow, by which neighbour genes with related functions (e.g. operons) happen to be transferred together and are then eroded slowly. These hypotheses may however be distinguished by analysing the historical record of evolutionary events that led to the clustering of co-functioning genes.

Most genes have complex histories, marked by many events of gene duplication, loss and, especially in the case of micro-organisms, horizontal transfers. The set of events affecting each homologous gene family in the pangenome under scrutiny can be summarized into an evolutionary scenario, which can be seen as the path of gene evolution within and across branches of the tree of species. Evolutionary scenarios can be inferred by comparing the phylogenetic history of genes and that of species, and by reconciling their discordances through the explicit inference of events of duplication, transfer and loss (Doyon et al. 2011; Scornavacca et al. 2012). This in turn allows to reconstruct the incremental shaping of genome gene contents, from ancestral to contemporary genomes, and to try and deduce the functional and ecological consequences of these changes.

We used the Rhizobiaceae family as a model taxon, particularly focusing on the *At* clade for which we gathered a dataset of 22 strains from ten different species, including 16 newly sequenced genomes. We designed a new phylogenetic pipeline for estimation of ancestral genomes that accounts for events of horizontal transfer and duplication of genes. Applied to our dataset, this approach estimates blocks of co-transferred and co-duplicated genes, allowing us to test hypotheses on how co-functioning gene clusters were formed. Comparing the level of functional co-operation of genes within blocks of co-transferred clade-

specific genes to the expectation under a neutral model of horizontal gene transfer (where genes are randomly picked from the donor genome) shows that clade-specific genes are more functionally related than expected. This supports the hypothesis by which the domestication of at least some clade-specific genes results from ecological selection.

Our reconstructed pangenome history – from single gene trees with transfer and duplication events to blocks of co-evolved genes and functional annotations– is compiled in an integrative database, Agrogenom, which can be visualized and queried through an interactive web interface accessible at http://phylariane.univ-lyon1.fr/db/agrogenom/3.

Methods

Bacterial Culture experiments.

Bacterial growth was analysed in the presence of phenylacetate (5mM) using a Microbiology Bioscreen C Reader (Labsystems, Finland) according to the manufacturer's instructions. *Agrobacterium* strains grown overnight in AT medium supplemented with succinate and ammonium sulfate were inoculated at an optical density at 600 nm (OD_{600}) of 0.05 in 200 µl AT medium supplemented with appropriate carbon and nitrogen sources in Bioscreen honeycomb 100-well sterile plates. The cultures were incubated in the dark for 3 days at 28°C with shaking at medium amplitude. Growth measurements (OD_{600}) were obtained at 20-min intervals.

Genome sequencing and assembly. Genomic DNAs of the 16 *At* strains (Table 1) prepared with the phenol-chloroform method were used to prepare libraries with DNA sheared into inserts of median size of 8 kb. Raw sequence data were then generated using 454 GS-FLX sequencer (Roche Applied Sciences, Basel, Switzerland) with a combination of single-read (SR) and mate-pairs (MP) protocols, that yielded coverage ranging from 6.5X to 11X and from 5X to 8X, respectively (Table S1). Genome sequences were then assembled with Newbler version 2.6 (Roche Applied Sciences, Basel, Switzerland), using 90% identity and 40-bp thresholds for alignment of reads into contigs and the '--scaffold' option to integrate duplicated contigs into the scaffold assembly. Pseudo-molecules (chromosomes and plasmids) regrouping scaffolds were manually created on the basis of plasmid profiles obtained from Eckhart gels (data not shown) and minimizing rearrangements between closely related genomes considering alignments of obtained with NUCmer program from MUMMER package version 3.0 (Kurtz et al. 2004). Genome sequences were then annotated with the MicroScope platform (Vallenet et al. 2013) and made available through the MaGe web interface (www.genoscope.cns.fr/agc/microscope) or the European Nucleotide Archive (http://www.ebi.ac.uk/ena/data/view/<ACCESSION NUMBERS> with accessions starred in Table 1).

Genomic sequence dataset. The study focused on the *Agrobacterium* biovar 1 species complex (*At*) with an original dataset of 16 new genomes along to six others publicly released (Goodner et al. 2001; Wood et al. 2001; Li et al. 2011; Ruffing et al. 2011; Wibberg et al. 2011; Hao, Lin, et al. 2012; Hao, Xie, et al. 2012).

These 22 genomes cover 10 closely related but genomically differentiated species (G1 to G9 and G13), with up to five isolates per species. The dataset also includes every genome publicly available for the Rhizobiaceae at the time of the database construction (spring 2012), and more distant relatives from the Phyllobacteriaceae and Rhodobiaceae family (Table 1; Figure S1).

Homologous gene family database. From the 47 complete genome sequence dataset, we built a database of homologous gene families on the model of Hogenom databases (Penel et al. 2009). All annotated protein coding sequences (CDSs) were extracted and translated into protein sequences on which a all-versus-all pairwise BLAST similarity search was performed to build a similarity network. Homologous gene families were derived from the network's connected components using HiFix (Miele et al. 2012). Gene family sequences were then aligned at the protein level using MUSCLE (Edgar 2004) and reverse-translated into CDS alignements with pal2nal (Suyama et al. 2006).

Reference species tree. To construct the reference species tree, 455 unicopy core gene families (i.e. families with exactly one copy per genome, listed Table S2) extracted from the Agrogenom database were used for 500 jackknife samples (draws without replacement) of 25 gene alignment sets, which were each concatenated and used to infer a maximum-likelihood (ML) tree using PhyML (Guindon & Gascuel 2003) (the same parameters as for gene trees, see S1 Text). The reference phylogeny was obtained by making the consensus of this sample of 500 trees with the CONSENSE algorithm from the Phylip package (Felsenstein 1993), and the branch supports were derived from the frequency of the consensus bipartitions in the sample (Figure S2). Alternative phylogenies were searched using the concatenate of the whole set of 455 universal unicopy families or from a concatenate of 49 ribosomal protein gene families (Table S3) to compute trees with RAxML (version 7.2.8, GTRCAT model, 50 discrete site-heterogeneity categories) (Stamatakis 2006).

Reconciliation of genome and gene tree histories. We computed gene trees using PhyML (Guindon & Gascuel 2003) for all the 10,774 gene families containing at least three genes (S1 Text) and rooted them using TPMS (Bigot et al. 2013) using the combo criterion, so that, knowing the species phylogeny, both the species multiplicity and the taxonomic depth of all subtrees are minimized. A root minimizing these criteria favours reconciliation scenarios more parsimonious in ancient gain (duplication and transfer) events and implied subsequent losses (Figure S3, step 1). As this criterion yields poor results in absence of ancestral duplications and presence of many transfers, we used another method to root unicopy gene trees (i.e. trees of gene families with at most one gene per genome): Prunier (Abby et al. 2010) was run for HGT detection (see below) and the root oferring the most parsimonious transfer scenario was retained. We then inferred an evolutionary scenario for each gene family, i.e. a mapping in the species tree of the presence/absence states of gene lineages and the origination, duplication and transfer events that created them. To do so, we reconciled the gene tree topologies with the species tree by assigning an event of either origination, duplication, transfer (ODT), or speciation to each of the 467,528 nodes found in the 10,774 gene trees. This

was achieved using a bioinformatic pipeline that combines several methods dedicated to the recognition of different signals of duplication and horizontal transfers; it is fully detailed in the Supplementary Text Sections 3 and 4, and summarized below and Table S4. Shortly, gene trees were processed as follows: likely duplication events were first located by looking for clades with multiple gene copies per species (Figure S3, step 2), marking 17,569 nodes as putative duplication from which 28,343 potential paralogous lineages emerge. We subsequently extracted subtrees in which every species was represented once, i.e. unicopy subtrees. In presence of lineage-specific paralogs ('in-paralogs'), we extracted the several possible combinations of co-orthologous gene copies (see Kristensen et al. 2011), producing different but overlapping unicopy subtrees (Figure S3, step 3; Suppl. Text section 4). Prunier, a parsimony-based method that takes into account the phylogenetic support of topological incongruences (Abby et al. 2010), was run on the unicopy subtrees to detect replacing transfer events at branches with statistically significant (SH-like support > 0.9) topological conflict (Figure S3, step 3). These reconciliations of (potentially overlapping) local subtrees yielded a total of 22,322 phylogenetically supported transfer events, which were mapped back to the gene trees (Figure S3, step 4). When several alternative (possibly conflicting) reconciliation scenarios were generated by independent inferences on overlapping lineage subtrees ("replicates"), the most likely scenario were chosen based on how many similar events were inferred in neighbouring gene families (Figure S3, step 5), favouring the events involved in the largest block events (see “Block event reconstruction” section below). Remaining topological incongruences may involve branches with phylogenetic support too low for Prunier to propose a transfer event, but could nonetheless be explained more parsimoniously with transfers than with duplications and losses; we thus used the taxonomic incongruence algorithm from (Bigot et al. 2013) to identify 1,899 conflicting branches as the place of additional transfer events, allowing a decrease of 10,229 counts of duplication events (Figure S3, step 6). Having obtained a final estimate of the location of duplications and horizontal transfers leading to the emergence of new gene lineages, we could define subfamilies of orthologs nested in homologous gene families (Figure S3, step 6). Finally, we used the Wagner parsimony algorithm implemented in the program Count (Csűrös 2008) to estimate scenarios of orthologous subfamily evolution, where transfers can be inferred to explain heterogeneous profiles of gene occurrence, leading to the detection of 19,553 additional transfer events (Figure S3, step 7). The illustrated description and programatic details of the reconciliation pipeline used in this studies are available at:
https://github.com/flass/agrogenom/blob/master/pipeline,
and intermediary input/ouput files and datasets are available at:
https://figshare.com/projects/Ancestral_genome_reconstruction_reveals_the_history_of_ecological_diversification_in_Agrobacterium/20894.

Coordinates of Origination, Duplication and Transfer events in the species tree.

Transfer events are characterized by the location of both donor and receiver ancestor nodes in the species tree (further referred to as “event coordinates”), which specifies the direction of the transfer; gene origination or duplication events are only characterized by their location at an ancestral node in the species tree. The

inference of co-events (events that involved sevral genes, see “Block event reconstruction” below) relies on the detection of similar events between gene families, i.e. events with the same coordinates. However, this can be challenging as independent evolution of genes after a co-event, for instance different histories of loss after a common ancestral gain by co-transfer, may leave very different patterns in the respective gene trees. The right count and coordinates of loss events are notoriously hard to estimate as there are many possible combinations of loss events for a fixed set of ODT events, with little information – only gene absence, i.e. missing data – to inform a choice. It follows that independent gene family scenario inferences – typically, if one applies a criterion of parsimony on the count of loss events subsequent to a gain by transfer, the transfer coordinates will be estimated as the last common ancestor of the species represented in the recipient clade – would often lead to different coordinate estimates for the same co-event (Figure 1A). To achieve a higher sensitivity in detecting similar events, we thus leave undetermined the count and location of loss events. This results in degrees of freedom on the ODT scenarios (further referred to as the uncertainty of the scenario), with several connected branches of the species tree on which ODT events could equally have happened (Figure 1 A).

Block event reconstruction. We define block events as unique ODT events that involved a block of several contiguous genes in an ancestral genome (‘ancestral block event’); by extension, ‘leaf block events’ refers to the extant blocks of genes descended from such an ancestral block event. We propose a greedy accretion procedure that links all leaf blocks to one common ancestral block, notably allowing to recover the unity of block events that may appear disrupted in individual genomes. The complete algorithm for block event reconstruction is described in the Supplementary Text, section 5 and summarized here. Blocks of genes sharing similar evolutionary events were first sought using a greedy algorithm similar to that defined by Williams et al. (Williams et al. 2012). Leaf block events were built by iterative inclusion of genes whose lineages were marked by events with compatible coordinates, i.e. events with overlapping sets of possible location in the species tree (see above). For instance, genes from family 1 and 2 are neighbour in an extant species’ genome; a transfer event was inferred in family 1, so the reconciled tree of family 2 is scanned for events with compatible donor-recipient coordinates (Figure 1A). As one such similar event is found, a block event involving both families is created; the donor-recipient coordinate set for that co-event is then defined as the intersection of both single events’ coordinate sets. Block events can then be extended with either another compatible gene or a maximum of two 'gap' genes without such signal (Figure S4 A, B), or terminated. After termination of a leaf block, inner gap genes were checked for phylogenetic compatibility of their lineage with the scenario associated to the block event (Figure S4 C), i.e. that donor and receptor clades are not separated from each other in the gene tree by any strongly supported branches. When branches separate the clade pairs but only showed weak statistical support (‘SH-like’ aLRT [Guindon et al. 2010] branch support < 0.9), the hypothesis of the transfer event would not be rejected and the block event integrity was maintained. Conversely, when the gene tree of the gap gene carried a strong signal rejecting the transfer event, the original block event was split into two block events representing separate transfer events (Figure

S4 D).

The ancestral block events were then reconstructed by searching homology relationships between leaf block events, defined as the belonging of at least a pair of genes from each leaf block event to the same homologous gene family and the coalescence of their lineages in the corresponding gene tree to the same node annotated with the ODT event that charaterizes the leaf blocks (Figure 1 B, step 2). Ancestral block events were iteratively assembled from homologous leaf block events and their coordinates estimated by intersection of their members' coordinates (Figure 1 B, step 3). An ancestral block event can link several leaf block events from different extant genomes or from the same genome. This allows us to unify disjoint leaf blocks from the same extant genome as fragments putatively derived from the same co-event. Indeed, because of gene insertion/deletion or genomic rearrangement, the contiguity of genes descending from a same event can easily be disrupted. It follows that the gene content of homologous leaf block events can differ, and thus their jointly estimated event coordinates can differ too. The leaf block homology relationship is supposed transitive, but due to these potential gene content differences, incompatibilities may arise during the iterative accretion of leaf block events into ancestral events; in that case a heuristic is used to resolve the conflict and distribute the leaf blocks in a number of self-compatible ancestral blocks (see Supplementary Methods, section 5). Block events were investigated for origination (O), duplication (D) and transfer (T) events, but not for losses (L). This is because of the higher rate at which actual convergent loss may occur (Kuo et al. 2009; David & Alm 2011; Szöllősi et al. 2012), and the larger solution space of loss scenarios leading to a higher risk of non-specific aggregation of unrelated loss events based on too uncertain event coordinates. For a similar reason of high risk of false positives, block events were not investigated on deep, long branches of the species tree (N1, N2, N3) for O and D (2,586 and 2,934 events overlooked, respectively), where many events were annotated with undistinguishable coordinates while they possibly occurred separately in time. After all homology search, the coordinates of the block events are finally reduced to the most recent possible location in the species tree and subsequent losses were inferred accordingly to complete the reconciliation.

Detection of clade-specific genes from phylogenetic profiles. Clade-specific genes are defined as genes that were were gained by the clade ancestor and conserved since in all clade members. From the sub-division of homologous gene families into orthologous subfamilies (see above and S1 Text, section 4, step 6), we established the phylogenetic profile of presence or absence of each subfamily in extant and ancient genomes and identified contrasting patterns of clade-specific genotypes. Contrast is defined relative to a larger background clade in which the focus (foreground) clade is included, where foreground genomes show a pattern consistently opposite to that of all other genomes in the background clade. Background clades were chosen as those corresponding to the next taxonomic unit (genus, species complex, etc.) including the foreground clade. Possible subsequent transfer or loss events in the background clade can blur the contrasting pattern in phylogenetic profiles. Clade-specific genotypes were thus first identified by gain/loss events in the genome of the foreground clade's ancestor, and then filtered using a relaxed definition of specificity, i.e.

where the presence/absence contrast can be incomplete, with up to two genomes in the background clade sharing the foreground state.

Functional homogeneity of gene groups. To measure to which extant co-transferred genes showed coherence in the functions they encoded, we used measures of semantic similarities of the Gene Ontology (GO) terms annotated to the gene products. First, the GO annotations were retrieved from UniProt-GOA (http://www.ebi.ac.uk/GOA/downloads, last accessed February, 2nd, 2013) (Dimmer et al. 2011) for the public genomes, and a similar pipeline of association of GO terms to gene products was used to annotate the genomic sequences produced for this study: the results of several automatic annotation methods were retrieved from the PkGDB database (Vallenet et al. 2013) : InterProscan, HAMAP, PRIAM and hits of blastp searches on SwissProt and TrEMBL databases (as on the February, 5th, 2013), with a general cut-off e-value of 10e-10. GO annotations were then mapped to gene products using the mappings between those method results and GO terms as provided by Uniprot-GOA for electronic annotation methods (http://www.ebi.ac.uk/GOA/ElectronicAnnotationMethods, last accessed February, 12th, 2013) : InterPro2GO, HAMAP2GO, EC2GO, UniprotKeyword2GO, UniprotSubcellular_Location2GO. The annotation dataset was limited to the electronically inferred ones to avoid biases of annotation of certain model strains or genes. The obtained functional annotations of proteomes were analysed in the context of Gene Ontology term reference (Full ontology file downloaded at http://www.geneontology.org/GO.downloads.ontology.shtml, last accessed September, 2nd, 2013) (Ashburner et al. 2000). Functional homogeneity (*FH*) within a group of genes is defined as the average of the pairwise functional similarities between all gene products in the group, each of which is the average of pairwise similarities between all terms annotated to a pair of genes. Similarities were measured using *Rel* and *funSim* metrics (Schlicker et al. 2006; Pesquita et al. 2009). Computations were done using a custom Python package derived from AIGO package v0.1.0 (https://pypi.python.org/pypi/AIGO).

To assess if co-transfer of genes was associated with coherent functions, the *FH* of co-transferred gene blocks was compared to that of random groups of genes, obtained either by uniformly sampling (i.e. random drawing without replacement) individual (non-linked) genes or by sampling genomic windows of neighbour (linked) genes. *FH* were computed for all windows of neighbour genes around a replicon, and a sample of the same size was drawn for random combinations of non-linked genes. Because the size of the group of genes impacts strongly the computation of the similarity metrics, and because the density of annotations can vary among organisms and replicons (contiguous DNA mollecule), the distributions of *FH* were calculated by replicon and by group size. Note that the set of block of co-transferred genes is included in the set of all genomic windows, but that non-overlapping subsets were used for statistical comparisons. In turn, to test if functional coherence of a block of co-transferred genes impacted its probability of retention after transfer, we compared the *FH* of genes from two sets of ancestral block events: those where all consituent genes were conserved in all descendant leaf block events, and those where part of the genes were lost in some descendant leaf block events. To avoid biases linked to variation in age of the considered transfer events, this

comparison was made only for events that occurred in ancestors of species-level clades of *At.*

Agrogenom database. All data about genes (functional annotations, gene families), genomes (position of genes, architecture in replicons …), the species tree (nodes, taxonomic information), reconciliations (gene trees, ODT events), block events, inference analyses (parameters, scores …), and all other data relative to the present work were compiled in a relational database, Agrogenom, for which a web interface for is accessible at http://phylariane.univ-lyon1.fr/db/agrogenom/3/.

Results and Discussion

Genomic Dataset and Reference Species Tree. To explore the history of the Rhizobiaceae pangenome, we gatherred 47 genomes, from genera *Agrobacterium*, *Rhizobium*, *Sinorhizobium*/*Ensifer*, *Mesorhizobium*/*Chelativorans* and *Parvibaculum* into the Agrogenom database. These genomes contain 281,223 coding sequences (CDSs, or genes hereafter) clustered into 42,239 homologous gene families. Out of these families, 27,547 were singletons with no detectable homologs (ORFan families) and 455 were found in exactly one copy in all the 47 genomes (unicopy core gene families). Following the procedure of (Abby et al. 2012), a species phylogeny was inferred from the concatenation of unicopy core gene family alignments, using jackknife re-sampling of genes to compute branch supports (Figure S2). Significant support is obtained for all clades corresponding to previously described species: *S. melitoti*, *R. etli*, *R. leguminosarum* and in particular for *At* species G1, G8, G4, G5 and G7. In contrast, the support is low for the relative positioning of most strains within species, showing conflicting (or lack of) signal among concatenated genes. Within the *At* clade, groupings of higher order were also highly supported: G8 with G6 (hereafter named [G6-G8] clade), G5 with G13, ([G5-G13] clade), G1 with [G5-G13] ([G1-G5-G13] clade), G3 with [G1-G5-G13] ([G3-G1-G5-G13] clade), G7 with G9 ([G7-G9] clade), and G4 with [G7-G9] ([G4-G7-G9] clade). Only some deep splits such as the position of G2 and of [G6-G8] clade relative to the *At* root were not well supported (Figure S2). We compared this species tree toppology to two others obtained with alternative datasets (see Methods): all three methods yielded very similar results concerning the placement of the different genera and species (Figure S5), the main difference residing in the rooting of *At* within the Rhizobiaceae clade, and the placement of lone representatitve for species G2 and G3. Exploration of the pangenome-wide support for alternative hypotheses (see Supplementary Text, section 1; Figure S6) confirmed that the best topology is provided by the jackknife sample consensus tree presented Figure S2. A phylogeny reconstructed based on the genome gene contents show less appropriate to discriminate species, indicating a large quantity of HGT is occurring (Figure S7).

Reconciliation of gene and species histories. To infer the history of HGT and other macro-evolutionary events, we reconciled the topologies of gene trees and species tree, i.e. we assigned an event of either origination, duplication, transfer (ODT), or speciation to nodes of the gene trees, which combination as a gene family evolution scenario make gene and species histories consistent. We use a succession of heuristics

10

aimed at the reconciliation of gene trees with the species tree that is parsimonious in losses and transfers to estimate individual gene family evolution scenarios (Figure S3).

Out of the 467,528 nodes found in the rooted gene trees of the 10,774 families that contained at least three genes, our pipeline assigned a total of 7,340 duplication events (1.5% of all gene tree nodes) and 43,233 transfers (9.2%). The remainder of unannotated gene tree nodes correspond to speciation events (where the gene tree topologies locally follow the species tree) and originations (apparition of the gene family in our dataset, mapped at the root of the gene tree) (Table 2). Based on the estimated ancestral genome gene contents, we could distinguish additive transfers that bring new genes from those that replace already present orthologous genes, the latter accounting for a quarter of total transfers (9,271 events). Additive transfers contribute almost five times more than duplications to the total gene input in genomes (Table S5), showing that transfer is the main source of gene content innovation in *At*.

Identification of co-events involving neighbour genes leads to a more parsimonious genome-wide scenario. Large-scale comparative genomics analyses have revealed that insertions in genomes typically comprise several consecutive genes, indicating that blocks of genes can evolve in linkage across genomes (Vallenet et al. 2009). Yet, ODT scenarios are generally evaluated for each gene tree independently of its neighbours (Makarova et al. 2006; Kettler et al. 2007). This is problematic because a scenario may be optimal (e.g., more parsimonious) for a gene alone, but sub-optimal in a model where genes can be part of the same ODT event (Figure 1). We developed a procedure to identify blocks of genes that likely co-evolved through the same event, based on the compatibility of their coordinates in the species tree (see Methods).

By assembling compatible ODT events from individual reconcilations of neighbour genes, we inferred 'block events', i.e. unique events involving blocks of co-evolved neighbour genes (Figure 1B,C). Pangenome-wide, we found numerous such block events in *At* genomes, with 17.5% of transfers and 13.3% of duplications involving at least two genes (Table 2). Several thousands of transfer events were infered to involve 2 to 6 genes, and a few hundreds to span a dozen or more consecutive genes in extant genomes (Figure S8 A). Moreover, reconstructed blocks of ancestral genes that we estimated to have been transferred between ancestral genomes (‘ancestral block events’) often appear to have been larger than their extant counterparts (Figure S8 B), indicating that rearrangements and partial losses in descendant genomes have frequently dismantled the syntenic blocks involved in ancient transfers.

Remarkably, factorizing those ODT events that, taken individually, would appear as convergent events into unique co-events dramatically changed the relative frequency of event types that were estimated to shape the pangenome: relative to scenarios based on a criterion of loss parsimony applied to single gene histories independently, block event scenarios resulted in the decrease of 13,421 ODT events, most of them transfer (10,978) and an increase of 2,896 loss (L) events (Table 2). The count of additional losses is however certainly over-estimated, because block events of gene loss must have occurred, but we did not intend to factorize loss events in this study (see Methods).

This difference in the estimated number of gene losses is due to the frequent under-estimation of the age of

the event when considering scenarios for individual gene families only, relative to joint scenarios for several gene families (Figure 1 A). As ODT events are thought to be less frequent than gene loss (L) events, and because the more complex pattern of transfers (characterized by a donor and a recipient) makes it less likely for T events with similar coordinates to happen convergently in neighbour genes (without hypothesis of linkage), factorizing similar ODT events for neighbour genes appears a reasonable approach to obtain a pangenome-wide scenario that is much more parsimonious in the total number of all kinds of events, i.e. ODTL events.

Inferred genome histories suggest selection for new genes in ancestors of key *At* lineages. Our inferred history of gain and loss in ancestral genomes of *At* showed heterogeneous dynamics across the species tree. First, we observe that the estimated genome sizes were significantly lower in estimated ancestral genomes than in extant genomes (Figure 2, Table S5). For instance, the reconstructed genome gene content, or gene repertoire, of the *At* clade ancestor contains around 4,500 genes, when extant genomes have an average size of 5,500 genes. This difference of 1,000 genes corresponds approximately to the number of genes recently gained along the terminal branches of the species tree (Figure 2), indicating the presence in contemporary genomes of a large polymorphism of gene presence/absence.

The variations of estimated gene repertoires showed significant relationships with the evolutionary distances in the species tree, indicating that on the long run, rather steady evolutionary processes were operating in these genomes. For instance, the length of the branch leading to the ancestor best explained the quantity of genes gained and lost by an ancestor (linear regression, r^2 = 0.59 and 0.32 for gains and losses, respectively), although removing the extreme point of node N35 (i.e. the G1 species ancestor) drops the correlations (r^2 = 0.27 and 0.28) (Figure S9 A, B). Interestingly, the quantity of genes gained by an ancestor and subsequently conserved in all members of the descendant clade, i.e. clade-specific genes, was robustly explained by the age of the ancestor (r^2 = 0.39, or 0.41 when removing N35) (Figure S9 F). This relationship was better described by a decreasing exponential regression (r^2 = 0.51, or 0.50 when removing N35), which reflects a process of 'survival' of genes in genomes through time (Figure 3). Alternatively, these trends could result from a systematic bias in our reconstruction procedure, for instance due to the fact that block event reconstruction tends to place gene gains higher in the species tree than single-gene family reconstruction would (Figure 1A), and thus results in more frequent inferrence of subsequent losses in older ancestors.

We identified outlier genomes in this putative process of 'gene survival', as the nodes having the largest residuals in the exponential regression (out of the 95% confidence interval). They were, in a decreasing order of excess of conservation relative to their age, the ancestors of [G6-G8], G1, G5, [G5-G13], G8 clades and those of subclades of G4 and G7 (Figure S9 F; Figure S10). These excesses of conservation do not systematically reflect a particular excess of gains in the ancestors: ancestors of G1 and G8 (nodes N35 and N32) have indeed gained more genes than predicted by their respective branch lengths, but on the contrary ancestors of [G6-G8], [G5-G13] and G5 (nodes N27, N34 and N39, respectively) have rather lost genes in excess (Figure S9 C, D). In the latter cases, the excesses of conserved gains may thus stem from a fixation

bias like natural selection for new genes. The outliers that fall above this trend – those clades that conserved more genes than predicted by their age – all belong to [G1-G5-G13] and [G6-G8] (Figure S10). The higher rate of conservation in these clades is indicative of a higher proportion of genes having been under purifying selection since their ancestral acquisitions, i.e. having been domesticated.

Clade-specific genes conserved over long times are likely providing a strong adaptive feature to their host organism. A new adaptive trait can improve an organism's fitness by increasing the differentiation of its ecological niche relative to cognate species, thus allowing it to escape competition. This emmergence of a new ecotype – an ecologically differentiated lineage – can for instance happen through a gain of function (e.g. via an additive HGT) allowing the exclusive consumption of a resource (Lassalle et al. 2015) or the change in relative reliance on a set of resources (Kopac et al. 2014). Spread of such niche-specifying trait to close relatives of the ecotype should be counter-selected (Cohan & Koeppel 2008) and their occurrence is thus expected to be restricted to the descendants of the ecotype, i.e. to be clade-specific. Recognizing such adaptive traits among clade-specific genes is thus the key to the understanding of the unique ecological properties of a bacterial clade.

Clusters of clade-specific genes are under purifying selection for their collective function. Niche-specifying traits are expected to provide higher differential fitness if they are less likely to be already present in, or independently acquired by, competing relatives. Hence, best candidates for niche-specifying traits consist of novel and complex sets of biochemical functions that do not rely on pre-existing functions. In such a case, it is crucial that the complete set of underlying biochemical functions is gained at once to provide any advantage. Such an event can typically happen with the co-transfer of a complete operon. In a previous study focused on G8 genomes (Lassalle et al. 2011), we observed that clade-specific genes tend to occur in clusters of genes with related biochemical function. This apparently non-random pattern suggests that co-transferred groups of genes collectively coding a function have been selected amongst incoming transferred genes, either by positive selection upon reception, or afterwards by negative (purifying) selection against the destruction of the group by rearrangement or partial deletion. This putative signature of selection made clusters of co-functioning clade-specific genes good candidates as niche-specifying determinants (Lassalle et al. 2011).

Yet, it is well known that bacterial genomes are organized in functional units such as operons, super-operons, etc. (Rocha 2008), and the co-transfer of cooperating genes could neutrally result from the functional structure of the donor genomes. However, the segments of DNA that are transferred are most probably taken randomly from the donor genomes (apart from the special case of genes coding their own mobility). Thus, under a neutral model, co-transferred genes should not always be co-functioning, and the probability at which a transferred fragment spanned a functional element like an operon would resemble that of any similarly sized fragment of the donor genome.

To test whether clustering of functionally related clade-specific genes results from selection, we designed tests that assess the relation between transfer history and biological function of genes. To do so, we define the degree of functional homogeneity (*FH*) of genes within groups of neighbour genes based on their Gene

Ontology annotation (see Methods). First, we checked that groups made of *n* genes each taken at random in the genome (physically distant genes) had lower *FH* than groups of *n* neighbour genes (taking all possible gene windows of *n* genes), confirming that *FH* captures the functional structure of a genome (Figure 4 A).

We then compared random groups of neighbour genes without a shared transfer history to blocks of transferred genes of the same size. The distribution of *FH* shows that while in general blocks of co-transferred genes gather genes that do not encode related functions or for which functional annotations are insufficient (FH ~ 0), a minor fraction presents intermediate to high functional relatedness (e.g. in G4-B6 genome, secondary modes at *FH* ~ 0.35 and *FH* ~ 0.75, Figure 4 A). Blocks of co-transferred genes had significantly higher *FH* than random groups in 45/49 significant tests preformed on independent combination of genomes and block sizes (Figure 4 A, C). This shows that fixation of transferred blocks of genes in genomes is biased towards blocks that code functional partners in a biological process. This observation supports the hypothesis of positive selection favouring the fixation in a recipient genome of those transferred genes that can immediately provide a selectable function. It is also compatible with the model of 'selfish operon' proposed by Lawrence and Roth (Lawrence & Roth 1996), as transfer followed by selection for readily functional multi-genic traits would lead to the prevalence in host genomes of genes clustered into tightly linked functional units.

In addition, we observe that among the groups of genes acquired by transfer, those that were conserved in all descendants of the recipient ancestors had more coherent annotated functions than non-conserved ones (11/13 significant tests positive, Figure 4 B, D). The hypothesis of conserved co-transferred genes encoding more related function than non-conserved ones was previously proposed based on manual inspection of the functional relatedness of a few transferred operons in *E. coli* (Homma et al. 2007) or the metabolic flux coupling of spatially clusterred transferred genes (from any origin) in Gammaproteobacteria (Dilthey & Lercher 2015). The present study presents a first quantitative estimation of functional relatedness within blocks of co-transferred genes, and provides a statistical argument for purifying selection enforcing their collective conservation in genomes. This supports our initial hypothesis that clusters of clade-specific genes participating to a same pathway, which are more likely to carry the sufficient information to encode a new adaptive trait, were under continued selection since their acquisition. It follows that the adaptations that characterize the ecological niche of a clade should be revealed through the identification of the genes specifically conserved in a clade, and notably those grouped in clusters with related functions.

Identification of clade-specific genes in *A. tumefaciens* key clades. We thus explored the histories of gene gain and loss in the clades of *At* to identify synapomorphic presence/absence of genes in *At* clades. We used an automated method for recognition of profiles of contrasted occurrence of genes between sister clades, by spotting ancestral gene gains or losses that resulted in conserved presence or absence in the descendant clade (see Methods). Doing so, we could account for convergent gains/losses of orthologous genes in distant clades, notably in cases of a transfer from one clade ancestor to another; this allowed us to show the specific sharing of genes between non-sister species of *At*. Listings of clade-specific genes of those key *At c*lades can

be found in S1 Dataset, or can be browsed on Agrogenom database website http://phylariane.univ-lyon1.fr/db/agrogenom/3/ (Figure 5). Generally, clade-specific genes were often located in relatively large clusters encoding coherent biochemical functions or pathways, which are summarized in Table S6 and hereafter numbered with the AtSp prefix. Those clade-specific gene clusters often match transfer or origination block events as estimated above (S1 Dataset), although often with limited coverage or with several transfer blocks mapping to a single clade-specific cluster. This suggests block gain events are likely to cluster at the same loci. Alternatively, it could indicate the limitation of our search procedure in face of the complexity of the gene histories, with different patterns of multiple consecutive transfers in different gene families preventing recognition of their common history. Full description of the biochemical functions encoded in these clade-specific gene repertoires can be found in the Supplementary Material (Supplementary Text section 7). A subset of clades of the *At* phylogeny, including species G1, G8, G4 and G7, are represented by several closely related extant genomes, and for this reason were particularly amenable for the accurate definition of clade-specific gene repertoires. For these, chromosomal maps of species-specific genes (Figures S11, S12, S13, S14) show they were located unevenly on the various replicons of *At* genomes, with a bias towards accumulation on the linear chromid (Lc), and an unexpected presence on the At plasmid (pAt) (Tables S6, S7).

Secondary replicons of Agrobacterium genomes bear clade-specific innovations. Rhizobiaceae present complex genomic architectures composed of a primary chromosome and a secondary chromosome or megaplasmid bearing essential genes, called chromid (Harrison et al. 2010), and a variable complement of plasmids of various sizes (Young et al. 2006). More specifically, the chromid of the *Agrobacterium* genus (Mousavi et al. 2015; Ormeño-Orrillo et al. 2015), which includes the *At* clade, is linear (Slater et al. 2009, 2013) as the result of an unique ancestral event of linearization and thus constituting a synapomorphy of this clade (Ramírez-Bahena et al. 2014). Another general feature of *At* genomes is the frequent presence of a pAt, a megaplasmid which was for long referred to as the cryptic plasmid, for its role in the cell biology remains largely unknown. We found that different pAt types are restricted to certain genomic backgrounds, as they host gene clusters specific to the host genome's species (namely G1, G8, G4 and G7 species) or higher groups ([G6-G8] clade) (Figures S11, S12, S13, S14), interspersed with genes that are mostly strain-specific. It thus seems that pAts are core replicons of a majority *At* species. In addition, while many megaplasmids of the same *repABC* family are known to recombine intensely within species (Kumar et al. 2015; Epstein et al. 2012), the occurerence of clade-specific genes on the pAt and never on the other plasmids (pTi and smaller ones) suggests a existence of barriers to its transfer. Within Cohan's ecotype framework, we interpret this pattern as the presence of determinants of the species' ecological niche on this particular extra-chromosomal element, which selectively prevents its spread among closely related species (Cohan & Koeppel 2008). This suggests that – for most species of *At* – the pAt is probably essential in natural environments, which would qualify it as a *bona fide* chromid (Harrison et al. 2010). Deletion-mutant competiton experiments on related chromid pSymB (diCenzo et al. 2016) have demonstrated the chromid had a significant fitness contribution

15

to the bacterium in the plant rhizopshere (i.e. out of nodule symbiosis), suggesting the general importance of these megaplasmids in adaptation to the core ecological niche of the bacterium (Lassalle et al. 2015).

Clade-specific gene functions provide insights into the possible ecological speciation of clade ancestors. The nature of putative ecological specialization is not obvious for agrobacteria, which are ubiquitous soil-dwellers. The frequent co-occurrence in soil of different species of *Agrobacterium*, sometimes in the same micro-metric sample (Vogel et al. 2003), dictates under the competitive exclusion principle (Gause 1932) that they have distinct ecologies. It is known that some soils and/or host plant show preferential colonization by certain species (Costechareyre et al. 2010), and G2 members appear to be have developped a capcity towards opportunistic pathogenicity in human (Aujoulat et al. 2011), showing the existence of some kind of niche differentiation among *Agrobacterium* species, but the precise nature of environmental factors that underlile it is mostly still to decrypt. Because the clade-specific genes must encode what makes a clade's ecology to be distinct from that of its relatives (Lassalle et al. 2015), we explored the specific functional repertoire of At clades. Strikingly, in most clades, including species or higher-level groups, the sets of clade-specific genes recurrently presented the same classes of functions. These include the transport and metabolism of phenolic compounds, aminoacids and complex sugars, and the production of exopolysaccharides and siderophores, all of which can be related to the life of bacteria in the plant rhizosphere (Lassalle et al. 2011).

Among these, we can notably report the specific presence of a supernumerary chemotaxis regulation operon *che2* in species G1, which is uniquely linked with an array of genes with predicted functions involved in the catabolism of (possibly aminated) aromatic compounds (Table S6). This suggests G1 strains are able to specifically degrade certain – yet unknown – aromatic compounds, for which they might display specific tropism and/or induction of biofilm formation.

G8 species and [G6-G8] clade present a number of clade-specific gene clusters (Table S6), as previously reported (Lassalle et al. 2011), among which the largest are the ferulic acid degradation and siderophore biosynthesis operons, which have been recently reported to provide a growth advantage and to be expressed in a coordinated manner in a plant rhizosphere environment (Campillo et al. 2014; Baude et al. 2016), showing the joint participation of G8 lineage-specific genes in the adaptation to a plant-related specific ecological niche. Interestingly, the gain of a siderophore biosynthesis locus in the ancestor of [G6-G8] coincided with the loss of the locus coding biosynthesis of another siderophore, agrobactin, which is otherwise ubiquitous in – and unique to – the *At* clade. This conserved switch to a different pathway for iron-scavenging – a crucial function in iron-depleted plant rhizospheres – may provide a competitive advantage with respect to co-occurring agrobacteria.

The species group [G5-G13] specifically presents a phenylacetate degradation pathway operon (Table S6), which biochemical function was demonstrated *in vitro* (Figure S15). This discovery readily provides us with a specific biochemical test for identification of these species, and again hints to the particular affinity of agrobacteria with aromatic compounds that are likely to be found in plant rhizospheres.

Finally, the large cluster that encodes the nitrate respiration (denitrification) pathway, including *nir*,

nor, *nnr* and *nap* operons is absent from [G1-G5-G13] clade. More recently, this gene cluster was also lost by strains G9-NCPPB925 and G8-ATCC31749, and its presence in strain G3-CFBP6623 seems to result from later transfer from a mosaic of sources within *At*. Considering the absence of this super-operon in close relatives of *At* such as *A. vitis* and *R. leguminosarum*, it appears that it was likely acquired by the ancestor of [G2-G4-G7-G9-G6-G8] clade (node N21 on Figure 1), one of the two large clades that divide *At* complex. These strains possessing the denitrification pathway may be selectively advantaged under certain anaerobic or micro-aerophilic conditions, such as those met in certain soils and rhizospheres.

Species G1 and G8 present a particular case of genomic gene content convergence, as we found that they share 57 synapomorphic genes (Table S7 and S8), in most cases with phylogenetic support for transfer events between respective ancestors. These traits were previously hypothesized to provide key adaptation to the life in the plant rhizosphere of G8 (= *A. fabrum*, (Lassalle et al. 2011)). For instance, they share homologous genes involved in the biosynthesis of curdlan – a cellulose-like polysaccharide – and the biosynthesis of O-antigens of the lipopolysaccharide (LPS), both capsular components that may define attachment properties of the cell to the external environment (Table S6; Supplementary Text S1, section 6.1). Indeed, the LPS synthesized by homologous enzymes in *Brucella spp.* mediate a specific interaction with cells of a eukaryotic host (Vizcaíno et al. 2001). In addition, different G1 and G8's clade-specific genes are encoding similar functional pathways, i.e. metabolism of phenolic compounds and production of exopolysaccharides (Table S6).

This overlap of the niche-specifying gene repertoires of G1 and G8 species may cause the convergence of their ideal ecological niches, and thus lead to inter-species competition for resources. However, shared niche-specifying genes are combined to different sets of species-specific genes in each species' core-genome, with which epistatic interaction could induce strong divergence in their phenotype. Typically, even though the loci for biosynthesis of O-antigens of the LPS in G1 and G8 are highly similar (>93% amino acid identity in average for proteins of the AtSp14 locus, Figure S16) and probably produce a structurally equivalent compound, these species' regulation of biofilm production is likely different. Indeed, there are several regulatory genes specific to G1 genomes involved in chemotaxis/biofilm production regulation, such as the *che2* operon (cluster AtSp2) and hub signal-transducing protein HHSS ('hybrid-hybrid' signal-sensing, see S1 Text, section 6.1) found in cluster AtSp14 (Figure S11 and S16), and a sensor protein (cluster AtSp3) modulating c-di-GMP – a secondary messenger involved in the switch from motile to sessile behaviours. Those specific regulators are all found linked to G1-specific genes involved in phenolics catabolism or biofilm production. These latter genes may constitute the downstream regulatory targets of what seems to be a coherent regulation network controlling motility, biofilm production and degradation of phenolics; this potentially constitute a whole pathway for response to environmental conditions specific of the niche of G1, such as availability of phenolics as nutrients. Similarly, G8-specific genes of the AtSp26 cluster (Figure S12) are forming a regulatory island involved in the perception and transduction of environmental signals, including mechanosensitive channels and a receptor for phenolic compound related to

toluene (Lassalle et al. 2011).

Both species are thus likely to orchestrate the production of similar polysaccharides under different regulation schemes, involving the coordination of their expression with other specific traits – interestingly, in both cases the catabolism of (likely different) phenolics. Similarly, the coordinated expression of several clade-specific genes, resulting in conditional phenotypes has recently been observed in G8-C58 (Baude et al. 2016), strengthening the idea of the existence of an ecological niche to which G8 species is specifically adapted through the expression of a particular *combination* of specific genes. The partial hybridization of G1 and G8 specific genomes thus likely leads each species to tap the same resources in a different way, which should not induce significant competition between them. These species may then form guilds of relatives that exploit partitions of a largely common ecological niche (Lassalle et al. 2015), explaining why we can observe them co-occurring in soils (Vogel et al. 2003; Portier et al. 2006). Regular events of such inter-species exchange of niche-specifying may explain why exploration of the genome based only on the presence/absence pattern of homologs – and not their gain history, as done here – may yield indistinct patterns of clade-specific gene contents, as recently observed among *R. leguminosarum* genomic species (Kumar et al. 2015).

Conclusion

We developed an original method for the reconstruction of the history of all genes in bacterial genomes and applied it to the *Agrobacterium* biovar 1 species complex (*At*), revealing the dynamics of gene repertoire in this taxon. These dynamics were structured along the tree of species and within genomes, revealing signatures of purifying selection for genes specifically gained by major clades of *At*. Most of these were organized in large blocks of co-evolving genes that encode coherent pathways, a pattern which constitutes a departure from a neutral model of gene transfer in bacterial genomes. We thus consider these blocks of clade-specific genes as likely determinants of the clades' core ecology. Genes specific to each species and to the *At* species complex as a whole recurrently encoded functions linked to production of secreted secondary metabolites or extracellular matrix, and to the metabolism of plant-derived compounds such as phenolics, sugars and amino acids. These clade-specific genes likely constitute parallel adaptations to life in interaction with host plant roots, which suggest that ecological differentiation of *Agrobacterium* clades occurred through the partitioning of ecological resources available in plant rhizospheres. In the future, sampling of within-species diversity, coupled with population genomics approaches, could further reveal ecological properties of agrobacteria, including those that may be non-ubiquitous but dynamically maintained by recombination within species (Kashtan et al. 2014; Rosen et al. 2015). Gene co-evolution models, such as the one developed here, may be extend to the investigation of inter-locus linkage in populations of genomes (Cui et al. 2015). Such analyses could reveal complex interactions between molecular pathways that are under ecological selection, opening new ways towards the understanding of bacterial adaptation to the infinite diversity of micro-environments.

Acknowledgements

This project was supported by the French National Research Agency (ANR, http://www.agence-nationale-recherche.fr/) grant ECOGENOME (ANR-BLAN-08-0090) and ANCESTROME (ANR-10-BINF-01-01) and by AGROMICS grant from the ENVIROMICS challenge of the Interdisciplinary Mission of the French National Centre for Scientific Research (CNRS). This work was performed using the computing facilities of the CC LBBE/PRABI. The LABGeM (CEA/IG/Genoscope & CNRS UMR8030) and the France Génomique National infrastructure (funded as part of 'Programme Investissement d'Avenir' of the ANR, contract ANR-10-INBS-09) are acknowledged for support within the MicroScope annotation platform. We thank David Bryant and two anonymous reviewers for their thoughtful comments on the manuscript.

Availability of supporting data

The sixteen new genome sequences used in these projects were submitted to the EBI-ENA (www.ebi.ac.uk/ena) under the BioProjects PRJEB12180-PRJEB12196. Accession numbers for the corresponding replicon sequences are LN999991-LN999996, LT009714-LT009764 and LT009775-LT009780. Accession numbers of all genomic data used in this dataset are listed Table 1. All other relevant data (output of analyses) are available on Figshare at https://figshare.com/projects/Ancestral_genome_reconstruction_reveals_the_history_of_ecological_diversification_in_Agrobacterium/20894. Original software developed for this work are available at https://github.com/flass/agrogenom.

Competing interests

The authors have declared that no competing interests exist.

Authors' contributions

FL, XN and VD conceived and supervised the study. DC, DMu and LV cultivated the bacteria, prepared the samples and conducted biochemical tests. FL, RP, SP, TG and LG contributed code and software. FL and RP designed Agrogenom database. RP conceived Agrogenom web interface. DMo generated functional annotation data. AC and DV integrated data into the Microscope database. VB led the sequencing project. VB, FL and AD participated in the genome assembly. FL, TG and VD conceived the phylogenetic methods. FL implemented the phylogenetic methods and performed the statistical and genomic analyses. FL, LV, DMu, VD and XN participated in writing the manuscript.

List of abbreviations

At – *Agrobacterium tumefaciens* species complex

CDS – coding sequence

FH – functional homogeneity

HGT – horizontal gene transfer

HR – homologous recombination

HHSS – "hybrid-hybrid" signal-sensing protein

ODT – origination, duplication and transfer (events)

ODTL – origination, duplication, transfer and loss (events)

Cc – circular chromosomes

Lc – linear chromid

pAt – *At* plasmid

pTi – Tumor-inducing plasmid

Supporting Information

Figure S1. Phylogeny of 131 genomes of Alpha-proteobacteria.

Figure S2. Reference phylogeny of Rhizobiales history.

Figure S3. Bioinformatic pipeline for reconciliation of gene and genome histories.

Figure S4. Algorithm for construction of blocks of co-transferred genes.

Figure S5. Alternative reference tree topologies obtained with different methods.

Figure S6. Support for monophyly of groups in all gene trees.

Figure S7. Hierarchical clustering of *Rhizobiales* genomes according to their gene content.

Figure S8. Distribution of sizes of block events.

Figure S9. Gene gain, loss and conservation within *At* clade ancestors.

Figure S10. Residuals of negative exponential regression of clade age vs. conservation of gained genes.

Figure S11. Historical stratification of gains in the lineage of *A. sp* G1 strain TT111.

Figure S12. Historical stratification of gains in the lineage of *A. sp.* G8 (*A. fabrum*) strain C58.

Figure S13. Historical stratification of gains in the lineage of *A. sp* G4 (*A. radiobacter*) strain B6.

Figure S14. Historical stratification of gains in the lineage of *A. sp. G7* strain Zutra 3/1.

Figure S15. Growth curves of representative of *At* genomic species on phenylacetate.

Figure S16. Syntenic conservation of the AtSp14 cluster in G1, G8 and Brucelaceae.

Table S1. Statistics of the 16 new genome sequences.

Table S2. List of the 455 universal unicopy gene families.

Table S3. Matrix of presence/absence of the 49 ribosomal gene families in the 47 Rhizobiaceae genomes.

Table S4. Bioinformatic pipeline for homologous database construction and Gene tree/Species tree

20

reconciliation.

Table S5. Statistics of gains and losses per contemporary and ancestral genome and replicon.

Table S6. Location and functional description of clade-specific gene clusters in *A. tumefaciens* genomes.

Table S7. Summary of clade-specific genes in TT111 genome.

Table S8. Summary of clade-specific genes in C58 genome.

S1 Text. Section 1. Comparison of several hypotheses for the core-genome reference phylogeny. **Section 2.** Construction of Agrogenom database. **Section 3.** Reconciliation of gene trees with the species tree. **Section 4.** Gene tree reconciliations: detailed procedure. **Section 5.** Block event reconstruction: algorithms. **Section Section 6.** Clade-specific genes: insights into the ecological properties of clades. **Section 7.** Selected cases of large transfer events. **Section 8.** Secondary replicons of *Agrobacterium* genomes bear clade-specific innovations.

S1 Dataset. Lists of clade-specific genes per clade.

References

Abby SS, Tannier E, Gouy M, Daubin V. 2010. Detecting lateral gene transfers by statistical reconciliation of phylogenetic forests. BMC Bioinformatics.

Abby SS, Tannier E, Gouy M, Daubin V. 2012. Lateral gene transfer as a support for the tree of life. Proc. Natl. Acad. Sci. 109:4962–4967.

Ashburner M et al. 2000. Gene Ontology: tool for the unification of biology. Nat. Genet. 25:25–29.

Aujoulat F et al. 2011. Multilocus sequence-based analysis delineates a clonal population of *Agrobacterium* (*Rhizobium*) *radiobacter* (*Agrobacterium tumefaciens*) of human origin. J. Bacteriol. 193:2608–2618.

Baude J et al. 2016. Coordinated Regulation of Species-Specific Hydroxycinnamic Acid Degradation and Siderophore Biosynthesis Pathways in *Agrobacterium fabrum*. Appl. Environ. Microbiol. 82:3515–3524.

Bigot T, Daubin V, Lassalle F, Perrière G. 2013. TPMS: a set of utilities for querying collections of gene trees. BMC Bioinformatics. 14:109.

Bruen TC, Philippe H, Bryant D. 2006. A Simple and Robust Statistical Test for Detecting the Presence of Recombination. Genetics. 172:2665–2681.

Campillo T et al. 2014. Analysis of Hydroxycinnamic Acid Degradation in *Agrobacterium fabrum* Reveals a Coenzyme A-Dependent, Beta-Oxidative Deacetylation Pathway. Appl. Environ. Microbiol. 80:3341–3349.

Cohan FM, Koeppel AF. 2008. The origins of ecological diversity in prokaryotes. Curr. Biol. CB. 18:R1024-1034.

Cooper VS, Vohr SH, Wrocklage SC, Hatcher PJ. 2010. Why Genes Evolve Faster on Secondary Chromosomes in Bacteria. PLoS Comput Biol. 6:e1000732.

Costechareyre D et al. 2010. Rapid and Efficient Identification of *Agrobacterium* Species by recA Allele Analysis : *Agrobacterium* recA Diversity. Microb. Ecol. 60:862–72.

Csűrös M. 2008. Ancestral Reconstruction by Asymmetric Wagner Parsimony over Continuous Characters and Squared Parsimony over Distributions. In: Comparative Genomics. Nelson, CE & Vialette, S, editors. Lecture Notes in Computer Science Springer Berlin Heidelberg pp. 72–86.

Cui Y et al. 2015. Epidemic Clones, Oceanic Gene Pools, and Eco-LD in the Free Living Marine Pathogen *Vibrio parahaemolyticus*. Mol. Biol. Evol. 32:1396–1410.

Daubin V, Lerat E, Perrière G. 2003. The source of laterally transferred genes in bacterial genomes. Genome Biol. 4:R57.

David LA, Alm EJ. 2011. Rapid evolutionary innovation during an Archaean genetic expansion. Nature. 469:93–96.

Dimmer EC et al. 2011. The UniProt-GO Annotation database in 2011. Nucleic Acids Res. 40:D565–D570.

Doolittle WF. 2013. Is junk DNA bunk? A critique of ENCODE. Proc. Natl. Acad. Sci. 110:5294–5300.

Doyon J-P, Ranwez V, Daubin V, Berry V. 2011. Models, Algorithms and Programs for Phylogeny Reconciliation. Brief. Bioinform. 12:392–400.

Felsenstein J. 1993. *PHYLIP (Phylogeny Inference Package) version 3.5c*.

Fitch WM. 1971. Toward Defining the Course of Evolution: Minimum Change for a Specific Tree Topology. Syst. Zool. 20:406.

Friedman J, Alm EJ, Shapiro BJ. 2013. Sympatric Speciation: When Is It Possible in Bacteria? PLoS ONE. 8:e53539.

Gause GF. 1932. Experimental Studies on the Struggle for Existence I. Mixed Population of Two Species of Yeast. J. Exp. Biol. 9:389–402.

Gonzalez V et al. 2010. Conserved Symbiotic Plasmid DNA Sequences in the Multireplicon Pangenomic Structure of *Rhizobium etli*. Appl Env. Microbiol. 76:1604–1614.

González V et al. 2003. The mosaic structure of the symbiotic plasmid of *Rhizobium etli* CFN42 and its relation to other symbiotic genome compartments. Genome Biol. 4:R36–R36.

Goodner B et al. 2001. Genome sequence of the plant pathogen and biotechnology agent Agrobacterium tumefaciens C58. Science. 294:2323–2328.

Guindon S, Gascuel O. 2003. A Simple, Fast, and Accurate Algorithm to Estimate Large Phylogenies by Maximum Likelihood. Syst. Biol. 52:696–704.

Hao X, Xie P, et al. 2012. Genome Sequence and Mutational Analysis of Plant-Growth-Promoting Bacterium *Agrobacterium tumefaciens* CCNWGS0286 Isolated from a Zinc-Lead Mine Tailing. Appl. Environ. Microbiol. 78:5384–5394.

Hao X, Lin Y, et al. 2012. Genome Sequence of the Arsenite-Oxidizing Strain *Agrobacterium tumefaciens* 5A. J. Bacteriol. 194:903.

Harrison PW, Lower RPJ, Kim NKD, Young JPW. 2010. Introducing the bacterial ‘chromid’: not a chromosome, not a plasmid. Trends Microbiol. 18:141–148.

Homma K, Fukuchi S, Nakamura Y, Gojobori T, Nishikawa K. 2007. Gene Cluster Analysis Method Identifies Horizontally Transferred Genes with High Reliability and Indicates that They Provide the Main Mechanism of Operon Gain in 8 Species of Gamma-Proteobacteria. Mol. Biol. Evol. 24:805–813.

Kashtan N et al. 2014. Single-Cell Genomics Reveals Hundreds of Coexisting Subpopulations in Wild *Prochlorococcus*. Science. 344:416–420.

Kettler GC et al. 2007. Patterns and Implications of Gene Gain and Loss in the Evolution of Prochlorococcus. PLoS Genet. 3:e231.

Kopac S et al. 2014. Genomic Heterogeneity and Ecological Speciation within One Subspecies of *Bacillus subtilis*. Appl. Environ. Microbiol. 80:4842–4853.

Kumar N et al. 2015. Bacterial genospecies that are not ecologically coherent: population genomics of *Rhizobium leguminosarum*. Open Biol. 5:140133.

Kuo C-H, Moran NA, Ochman H. 2009. The consequences of genetic drift for bacterial genome complexity. Genome Res. 19:1450–1454.

Kurtz S et al. 2004. Versatile and open software for comparing large genomes. Genome Biol. 5:R12.

Lassalle F et al. 2011. Genomic Species Are Ecological Species as Revealed by Comparative Genomics in *Agrobacterium tumefaciens*. Genome Biol. Evol. 3:762–781.

Lassalle F, Muller D, Nesme X. 2015. Ecological speciation in bacteria: reverse ecology approaches reveal the adaptive part of bacterial cladogenesis. Res. Microbiol. 166:729–741.

Lawrence JG, Ochman H. 1997. Amelioration of Bacterial Genomes: Rates of Change and Exchange. J. Mol. Evol. 44:383–397.

Lawrence JG, Roth JR. 1996. Selfish operons: horizontal transfer may drive the evolution of gene clusters. Genetics. 143:1843–1860.

Li A et al. 2011. Genome Sequence of Agrobacterium tumefaciens Strain F2, a Bioflocculant-Producing Bacterium. J. Bacteriol. 193:5531–5531.

Makarova K et al. 2006. Comparative genomics of the lactic acid bacteria. Proc. Natl. Acad. Sci. 103:15611–15616.

Marri PR, Harris LK, Houmiel K, Slater SC, Ochman H. 2008. The Effect of Chromosome Geometry on Genetic Diversity. Genetics. 179:511–516.

Morrow JD, Cooper VS. 2012. Evolutionary Effects of Translocations in Bacterial Genomes. Genome Biol. Evol. 4:1256–1262.

Mousavi SA, Willems A, Nesme X, de Lajudie P, Lindström K. 2015. Revised phylogeny of Rhizobiaceae: Proposal of the delineation of *Pararhizobium* gen. nov., and 13 new species combinations. Syst. Appl. Microbiol. 38:84–90.

Ormeño-Orrillo E et al. 2015. Taxonomy of rhizobia and agrobacteria from the Rhizobiaceae family in light of genomics. Syst. Appl. Microbiol. 38:287–291.

Penel S et al. 2009. Databases of homologous gene families for comparative genomics. BMC Bioinformatics. 10:S3.

Pesquita C, Faria D, Falcão AO, Lord P, Couto FM. 2009. Semantic Similarity in Biomedical Ontologies. PLoS Comput Biol. 5:e1000443.

Portier P et al. 2006. Identification of genomic species in *Agrobacterium* biovar 1 by AFLP genomic markers. Appl. Environ. Microbiol. 72:7123–7131.

Ramírez-Bahena MH et al. 2014. Single acquisition of protelomerase gave rise to speciation of a large and diverse clade within the *Agrobacterium*/*Rhizobium* supercluster characterized by the presence of a linear chromid. Mol. Phylogenet. Evol. 73:202–207.

Rocha EPC. 2008. The Organization of the Bacterial Genome. Annu. Rev. Genet. 42:211–233.

Rosen MJ, Davison M, Bhaya D, Fisher DS. 2015. Fine-scale diversity and extensive recombination in a quasisexual bacterial population occupying a broad niche. Science. 348:1019–1023.

Ruffing AM, Castro-Melchor M, Hu W-S, Chen RR. 2011. Genome sequence of the curdlan-producing *Agrobacterium* sp. strain ATCC 31749. J. Bacteriol. 193:4294–4295.

Schlicker A, Domingues FS, Rahnenführer J, Lengauer T. 2006. A new measure for functional similarity of gene products based on Gene Ontology. BMC Bioinformatics. 7:302.

Slater S et al. 2013. Reconciliation of Sequence Data and Updated Annotation of the Genome of Agrobacterium tumefaciens C58, and Distribution of a Linear Chromosome in the Genus *Agrobacterium*. Appl. Environ. Microbiol. 79:1414–1417.

Slater SC et al. 2009. Genome sequences of three *Agrobacterium* biovars help elucidate the evolution of multichromosome genomes in bacteria. J. Bacteriol. 191:2501–2511.

Stamatakis A. 2006. RAxML-VI-HPC: Maximum Likelihood-Based Phylogenetic Analyses with Thousands of Taxa and Mixed Models. Bioinformatics. 22:2688–2690.

Szöllősi GJ, Boussau B, Abby SS, Tannier E, Daubin V. 2012. Phylogenetic modelling of lateral gene transfer reconstructs the pattern and relative timing of speciations. Proc. Natl. Acad. Sci. 109:17513–17518.

Touchon M et al. 2009. Organised genome dynamics in the *Escherichia coli* species results in highly diverse adaptive paths. PLoS Genet. 5:e1000344.

Vallenet D et al. 2009. MicroScope: a platform for microbial genome annotation and comparative genomics. Database J. Biol. Databases Curation. 2009:bap021.

Vallenet D. MicroScope Home - MaGe: Microbial Genome Annotation & Analysis Platform - MicroScope - Web Interface System & Specialized Databases for (re)Annotation and Analysis of Microbial Genomes. MicroScope. https://www.genoscope.cns.fr/agc/microscope/home/index.php (Accessed December 18, 2015).

Vallenet D et al. 2013. MicroScope--an integrated microbial resource for the curation and comparative analysis of genomic and metabolic data. Nucleic Acids Res. 41:D636-647.

Vizcaíno N, Cloeckaert A, Zygmunt MS, Fernández-Lago L. 2001. Characterization of a *Brucella* species 25-kilobase DNA fragment deleted from Brucella abortus reveals a large gene cluster related to the synthesis of a polysaccharide. Infect. Immun. 69:6738–6748.

Vogel J, Normand P, Thioulouse J, Nesme X, Grundmann GL. 2003. Relationship between spatial and genetic distance in Agrobacterium spp. in 1 cubic centimeter of soil. Appl. Environ. Microbiol. 69:1482–1487.

Volff JN, Altenbuchner J. 2000. A new beginning with new ends: linearisation of circular chromosomes during bacterial evolution. FEMS Microbiol. Lett. 186:143–150.

Wibberg D et al. 2011. Complete genome sequencing of *Agrobacterium* sp. H13-3, the former *Rhizobium lupini* H13-3, reveals a tripartite genome consisting of a circular and a linear chromosome and an accessory plasmid but lacking a tumor-inducing Ti-plasmid. J. Biotechnol. In Press, Uncorrected Proof.

Williams D, Gogarten JP, Papke RT. 2012. Quantifying Homologous Replacement of Loci between Haloarchaeal Species. Genome Biol. Evol. 4:1223–1244.

Wood DW et al. 2001. The genome of the natural genetic engineer *Agrobacterium tumefaciens* C58. Science. 294:2317–2323.

Young JPW et al. 2006. The genome of *Rhizobium leguminosarum* has recognizable core and accessory components. Genome Biol. 7:R34.

25

Figure legends and tables

Fig. 1: Gene-wise vs. regional reconciliation. A) Transfers inferred in reconciled gene trees 1 and 2 can be translated in several possible scenarios in the species tree that each involves different donor (Do) and receiver (Re) pairs (multiple arrows with question marks, uncertain scenarios). If each gene family is reconciled separately, the scenarios that place the ancestral receiver at the last common ancestor of extant recipient genomes are chosen because they are the most parsimonious in losses (crosses mapped on the species tree and "Local event count" in inset table). That way, the global scenario for the combined loci totalizes two transfers and no subsequent loss (inset table, "Combined event count"). If the transfer event coordinates are compatible (i.e. non-null intersection: Re:{N7, N11} ∩ Re:{N11, L} = Re:{N11}) between gene families, one can consider the possibility of the co-transfer of neighbour genes 1 and 2 as a common (Block) transfer event. By minimizing the total number of (co-)transfer events, a scenario can be chosen which is not necessarily the most parsimonious in losses for each gene. In this example, the global scenario for the combined loci which is the most parsimonious in transfer events totalizes one block transfer and one subsequent gene loss. B) Refinement of event uncertainties when building block events. Origination, duplication and transfer events are first inferred in each gene family separately (1); for the sake of clarity, the example shows only transfer events as arrows on branches of gene trees (top) and between branches of species trees (bottom). Compatible events affecting genes that are neighbour in at least one extant genome are aggregated into blocks (coloured frames) (2) and this approach is then repeated across genomes (vertical double arrows), thus reconstructing the events that occurred in ancestral genomes (3). Numbers in circles indicate the number of genes combined in a same event, stars indicate when aggregation of an event lead to the refinement of its coordinates (i.e. reduction of the set of possible locations of the event in the species tree).

Fig. 2: Ancestral genome sizes and gain/loss events. The tree is a subtree of that presented Figure S1, focusing on the *At* clade. Net gains (+) and losses (-) and resulting genome sizes (=) are indicated next to nodes. Disc at nodes schematically represent inferred ancestral genomes or actual extant genomes; surfaces are proportional to the genome size. Prevalence of events shaping the gene content are indicated by pie charts indicating the fraction of losses (red), gains by duplication (cyan), gains by transfer (blue) and gene conversions/allelic replacements (green). The relatively high number of event occurring at *At* root is related to the long branch from which it stems in the complete Rhizobiales tree (Fig. S1), which is not represented here.

Fig. 3: Retention of gained genes within *At* genomes follows a 'survival' model. Node 'N15' (the G1 species ancestor) is the strongest driver in the linear regression. Dark and light shaded areas respectively represent the 95% and 99% confidence intervals of the exponential model (solid blue line).

Fig. 4: Functional homogeneity of gene clusters. (A, B) Distribution of functional homogeneities (*FH*) of genes within clusters using representative plots comparing clusters of two genes in the B6 genome (a G4 member). (A) Comparison of functional homogeneities of groups of two genes taken in the B6 genome: randomly distant pairs (black), any pair of neighbour genes without common transfer history (blue) or pairs of co-transferred neighbour genes (red). (B) Comparison of functional homogeneities of pairs of co-transferred genes from families conserved in all G4 strains (green) or not conserved (red). (C, D) Distribution of *p*-values of Mann-Whitney-Wilcoxon sum of ranks test comparing the distributions of *FH* (made independently for all *At* genomes at all discrete block sizes) of (C) random windows of non co-transferred genes vs. blocks of co-transferred genes or (D) conserved vs. non-conserved blocks of co-transferred genes. Each point represents an observation from an extant *At* genome for a given size of groups of genes (on x-axis). Point colours indicate the higher-*FH* sample (as in A,B): (C) blue, *FH*(random windows) > *FH*(transferred blocks), (n = 29, 4 significant); red, *FH*(random windows) < *FH*(transferred blocks), n = 66 (45 significant) ; (D) purple, *FH*(non-conserved blocks) > *FH*(conserved blocks), n = 11 (2 significant) ; green, *FH* (non-conserved blocks) < *FH* (conserved blocks), n = 49 (11 significant). A test is considered significant at $p < 0.01$. Effective of tests in favour of one hypothesis or the other are counted over all independent tests made for each combination of *At* genomes and discrete block sizes.

Fig. 5: Snapshot of the Agrogenom web interface.
View of the *recA* gene family. (1) Reconciled gene tree; the orange diamond under the mouse cursor indicate a transfer event from G2-CFBP 5494 to G9-Hayward 0363. (2) Detailed annotation of the sequences at the tip of the tree, including locus tag (linking out to MaGe genome browser), chromosomal location, taxon name, database cross-references, etc. (3) Dynamic menu to adapt the level of displayed information. (4) Syntenic view in the genomic neighbourhoods of the focal gene family; homologs are sharing the same colour, defined in reference to a chosen sequence (indicated by the navigation arrows on the sides). (5) Blue frame indicates a block transfer event involving four gene families; this block appears dynamically when hovering the cursor above the transfer node in the gene tree. (6) Pop-up window with functional annotation and characteristics of a gene can be generated by double-clicking on the

gene; it contains the link to the gene tree of the gene's family. (7) Search menus: 'Advanced search' to get a gene family by its annotation; 'Gene Sets' to browse lists of genes: clade-specific genes, core genome, ancestral gene content, clade-specific gains/losses. (8) Alternative views of the family with projection on the species tree.

Table 1: List of 47 Rhizobiales strains used in this study.

Clade/Taxon	Strain name	NCBI Taxid	EMBL Sequence accession number	Nb. of genes
***Agrobacterium biovar 1* / *A. tumefaciens* species complex (*At*)**				
A. sp. G1	H13-3	861208	CP002248-CP002250	5345
	5A	1107544	AGVZ00000000	5518
	CFBP 5771	1183421	LT009762-LT009764*	5546
	S56	1183429	LN999991-LN999996*	5627
	TT111	1183430	LT009714-LT009717*	5856
A. sp. G2 (*A. pusense*)	CFBP 5494	1183436	LT009718-LT009722*	6013
A. sp. G3	CFBP 6623	1183432	LT009723-LT009726*	5378
A. sp. G4 (*A. radiobacter*)	B6	1183423	LT009758-LT009761*	5875
	CFBP 5621	1183422	LT009727-LT009729*	5330
	Kerr 14	1183424	LT009730-LT009734*	5870
	CCNWGS0286	1082932	AGSM00000000	4979
A. sp. G5	CFBP 6626	1183435	LT009735-LT009738*	5332
	F2	1050720	AFSD00000000	5321
A. sp. G6	NCPPB 925	1183431	LT009739-LT009744*	6139
A. sp. G7	NCPPB 1641	1183425	LT009775-LT009778*	6041
	RV3	1183426	LT009745-LT009747*	5182
	Zutra 3/1	1183427	LT009748-LT009751*	5685
A. sp. G8 (*A. fabrum*)	C58	176299	AE007869-AE007872	5639
	ATCC 31749	82789	AECL00000000	5535
	J-07	1183433	LT009752-LT009755*	5592
A. sp. G9	Hayward 0363	1183434	LT009779-LT009780*	4502
A. sp. G13	CFBP 6927	1183428	LT009756-LT009757*	4993
Allorhizobium				
Allorhizobium vitis	S4	311402	CP000633-CP000639	5389
Rhizobium sp.	PDO1-076	1125979	AHZC00000000	5340
Rhizobium				
R. rhizogenes	K84	311403	CP000628-CP000632	6684
R. etli	CIAT 652	491916	CP001074-CP001077	6109
	CFN 42	347834	CP000133-CP000138, U80928	6016
	CNPAF512	993047	AEYZ00000000	6544
R. leguminosarum bv. *viciae*	3841	216596	AM236080-AM236086	7263
R. leguminosarum bv. *trifolii*	WSM1325	395491	CP001622-CP001627	7001
	WSM2304	395492	CP001191-CP001195	6415
***Ensifer/Sinorhizob*ium**				
E. meliloti	1021	266834	AL591688, AE006469, AL591985	6234
	BL225C	698936	CP002740-CP002742	6354
	CCNWSX0020	1107881	AGVV01000000	6844
	AK83	693982	CP002781-CP002785	6510
	SM11	707241	CP001830-CP001832	7093
E. medicae	WSM419	366394	CP000738-CP000741	6213
E. fredii	HH103	1117943	HE616890-HE616899	6787
	NGR234	394	CP000874, CP001389, U00090	6366
Mesorhizobium/ Chelativorans				
M. alhagi	CCNWXJ12-2	1107882	AHAM00000000	7184
M. amorphae	CCNWGS0123	1082933	AGSN00000000	7075
M. australicum	WSM2073	7540353	AGIX00000000	5934
M. ciceri bv. *biserrulae*	WSM1271	765698	CP002447, CP002448	6264
M. opportunistum	WSM2075	536019	CP002279	6508
M. loti	MAFF303099	266835	AP003017, BA000012, BA000013	7281
Chelativorans sp.	BNC1	266779	CP000389-CP000392	4543
Parvibaculum				
P. lavamentivorans	DS-1	402881	CP000774	3636

*: accessions of strain genomes newly sequenced in this study.

Table 2: Origination, Duplication, Transfer and Speciation events inferred in reconciliations of the Agrogenom database.

Event type	Single gene events	Block events	(of size >1)	Difference after event integration into blocks
Originations	5,189	4,267	(667)	-922
Duplications	7,340	5,819	(778)	-1,521
Total transfers	43,233	32,255	(5,649)	-10,978
Replacing transfers †	9,271	-	-	
Additive transfers †	33,962	-	-	
Total ODT	55,762	42,341	(7,094)	-13,421
Implied losses	29,843	32,739	-	+2,896
Total ODTL	85,605	75,080	-	-10,525

O, origination; D, duplication; T, transfer; L, loss; ODT refers to the combination of all O, D and T events, ODTL also includes losses. †: Replacing and additive transfers are not distinguished in block events.

A.

Reconciliation scenarios projected on the species tree:

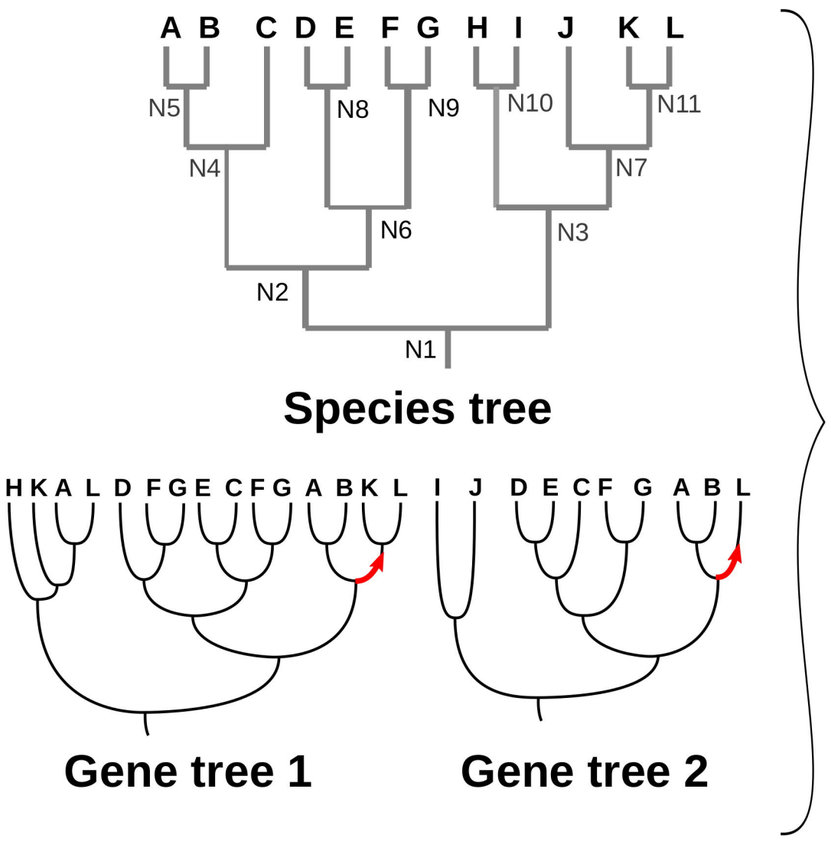

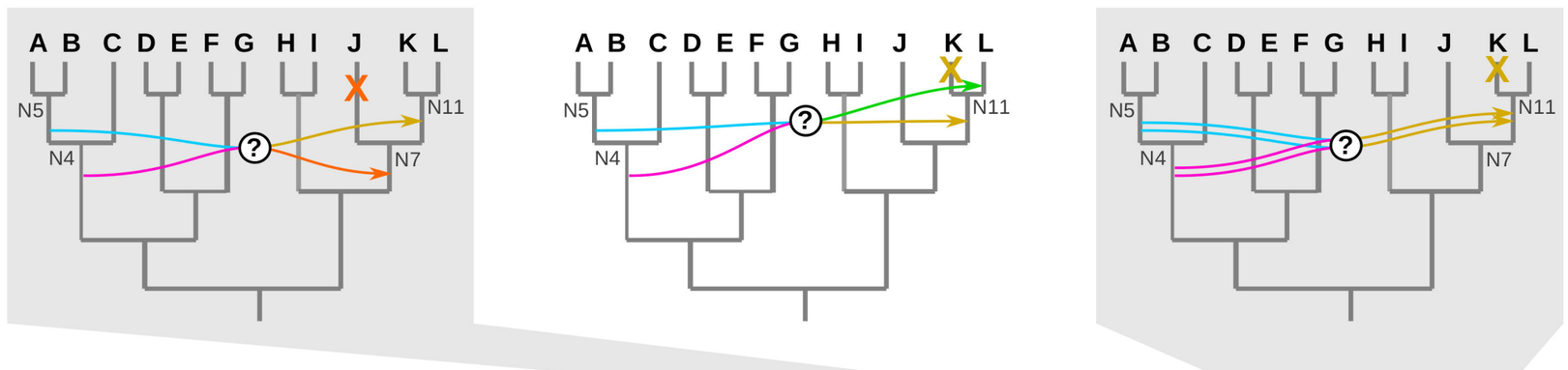

		Single gene 1		Single gene 2		Block (genes 1 & 2)	
Transfer coordinates		Do →	Re	Do →	Re	Do →	Re
	Possible	{N4, N5}	{N7, N11}	{N4, N5}	{N11, L}	{N4, N5}	N11
	LCA	N5	N11	N5	L	N5	N11
Local event count							
	Transfers	1		1		1	
	Losses	0		0		1	
Combined event count							
	Transfers	**2**				**1**	
	Losses	**0**				**1**	

B.

1) Reconstruction evolutionary events in gene families

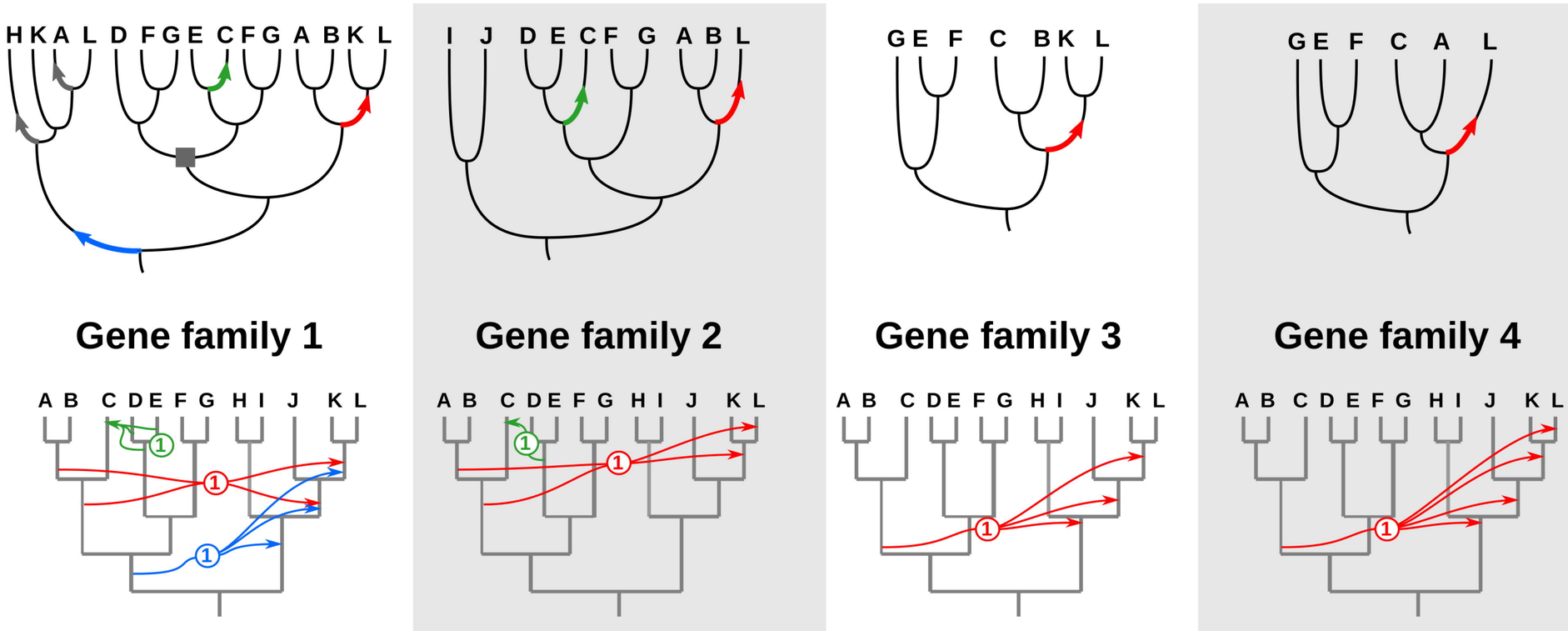

2) Reconstruction of block events in contemporary genomes

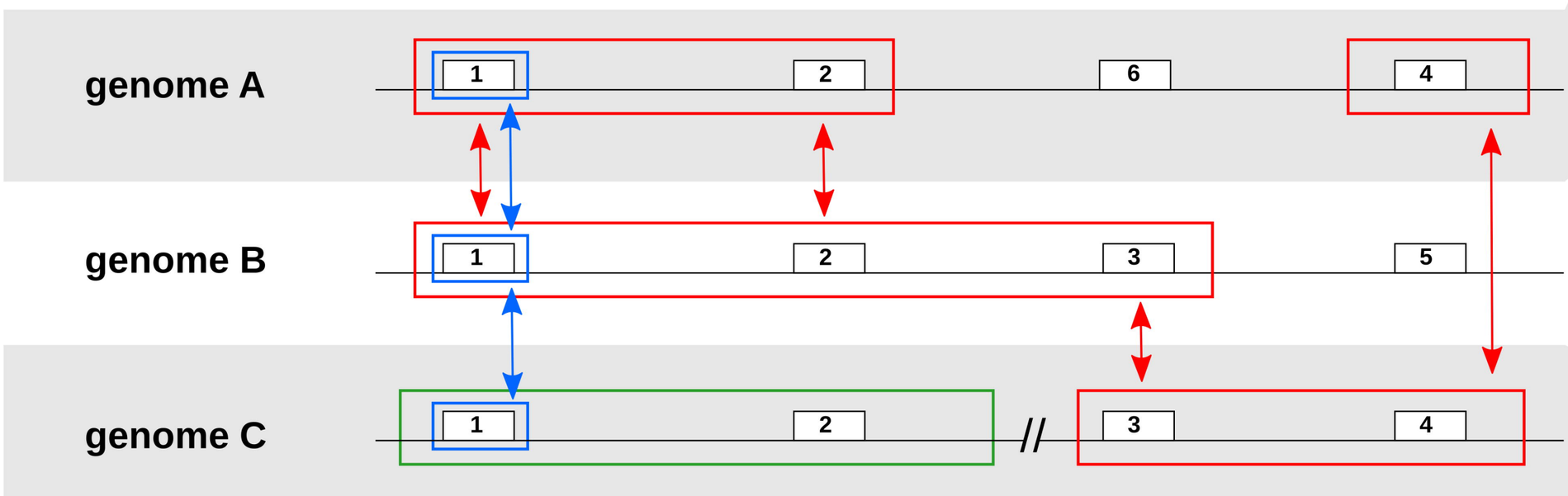

3) Reconstruction of ancestral block events

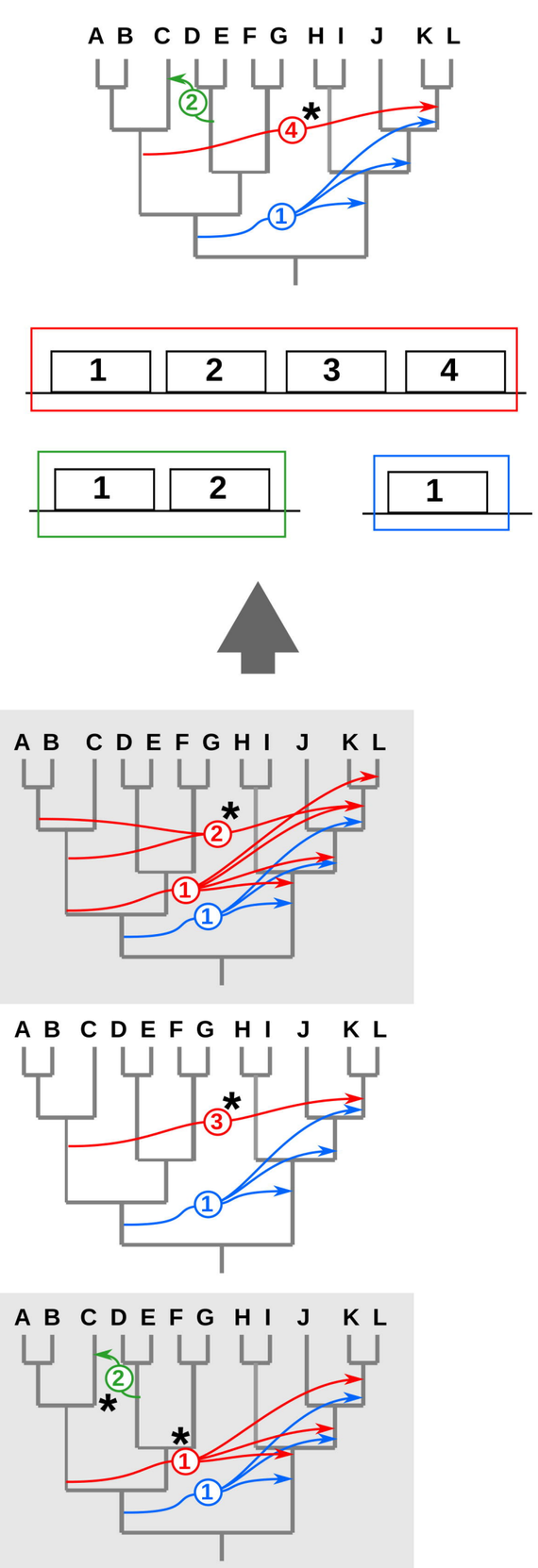

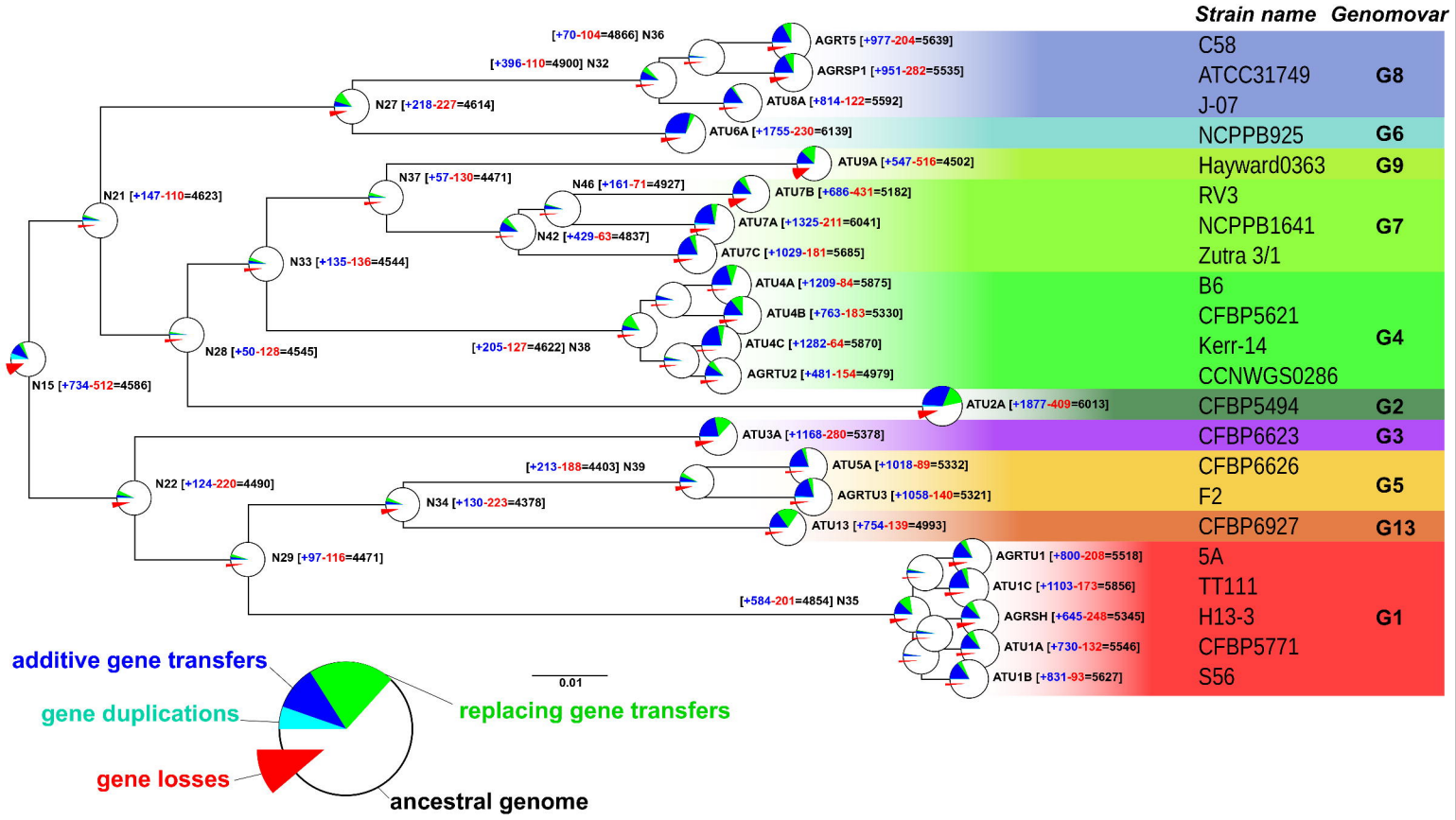
Strain name
Genomovar
[+70-104=4866] N36
AGRT5 [+977-204=5639]
C58
[+396-110=4900] N32
AGRSP1 [+951-282=5535]
ATCC31749
G8
N27 [+218-227=4614]
ATU8A [+814-122=5592]
J-07
ATU6A [+1755-230=6139]
NCPPB925
G6
ATU9A [+547-516=4502]
Hayward0363
G9
N37 [+57-130=4471]
N46 [+161-71=4927]
ATU7B [+686-431=5182]
N21 [+147-110=4623]
RV3
ATU7A [+1325-211=6041]
NCPPB1641
G7
N42 [+429-63=4837]
ATU7C [+1029-181=5685]
Zutra 3/1
N33 [+135-136=4544]
ATU4A [+1209-84=5875]
B6
ATU4B [+763-183=5330]
CFBP5621
ATU4C [+1282-64=5870]
Kerr-14
G4
N28 [+50-128=4545]
[+205-127=4622] N38
AGRTU2 [+481-154=4979]
CCNWGS0286
N15 [+734-512=4586]
ATU2A [+1877-409=6013]
CFBP5494
G2
ATU3A [+1168-280=5378]
CFBP6623
G3
[+213-188=4403] N39
ATU5A [+1018-89=5332]
CFBP6626
N22 [+124-220=4490]
AGRTU3 [+1058-140=5321]
F2
G5
N34 [+130-223=4378]
ATU13 [+754-139=4993]
CFBP6927
G13
N29 [+97-116=4471]
AGRTU1 [+800-208=5518]
5A
ATU1C [+1103-173=5856]
TT111
[+584-201=4854] N35
AGRSH [+645-248=5345]
H13-3
G1
ATU1A [+730-132=5546]
CFBP5771
ATU1B [+831-93=5627]
S56
0.01
additive gene transfers
gene duplications
gene losses
replacing gene transfers
ancestral genome

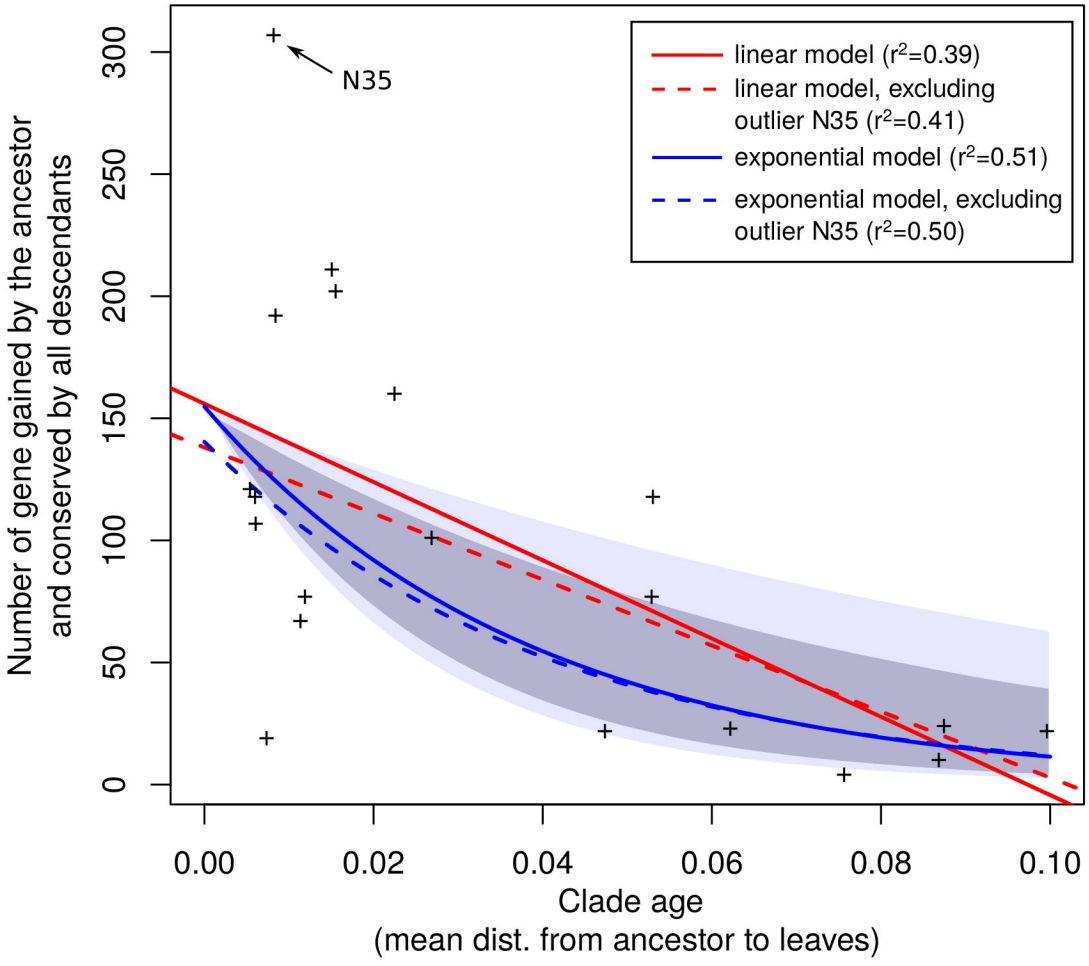
linear model (r^2=0.39)
linear model, excluding outlier N35 (r^2=0.41)
exponential model (r^2=0.51)
exponential model, excluding outlier N35 (r^2=0.50)
N35
Number of gene gained by the ancestor and conserved by all descendants
0
50
100
150
200
250
300
0.00
0.02
0.04
0.06
0.08
0.10
Clade age
(mean dist. from ancestor to leaves)

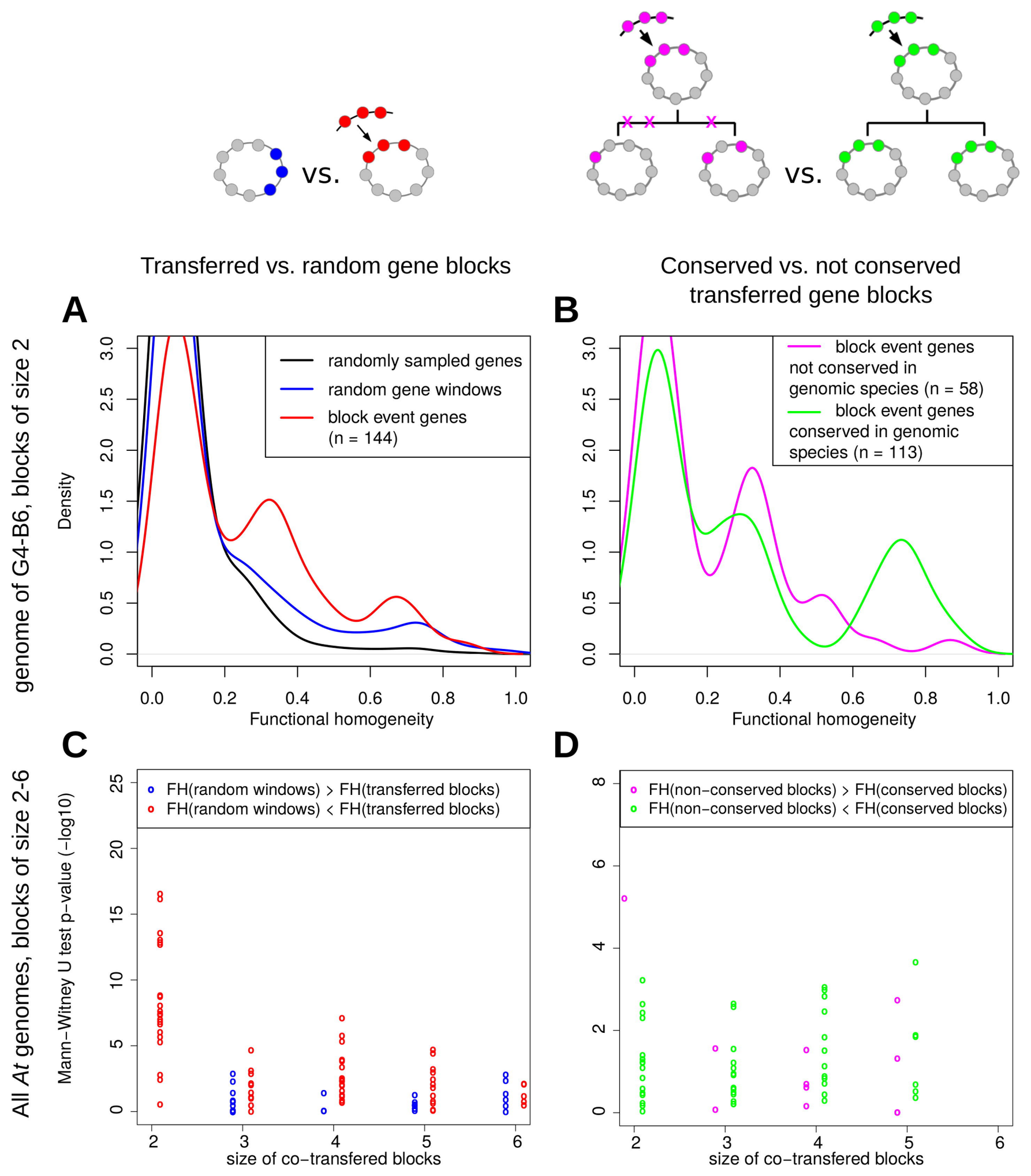
vs.
vs.
Transferred vs. random gene blocks
Conserved vs. not conserved transferred gene blocks
A
B
C
D
genome of G4-B6, blocks of size 2
All At genomes, blocks of size 2-6
randomly sampled genes
random gene windows
block event genes (n = 144)
block event genes not conserved in genomic species (n = 58)
block event genes conserved in genomic species (n = 113)
Density
Functional homogeneity
FH(random windows) > FH(transferred blocks)
FH(random windows) < FH(transferred blocks)
FH(non−conserved blocks) > FH(conserved blocks)
FH(non−conserved blocks) < FH(conserved blocks)
Mann−Witney U test p−value (−log10)
size of co−transfered blocks

Agrogenom3

Search | Advanced Search | Gene Sets | 7

reconciled phylogenetic tree | Taxonomic Tree | Taxonomic Rules | Species Tree | 8

phylogram | nodeSupport | Column Annotations | 3

1 2 4 5 6

SMc00760	chromosome 1	Sinorhizobium meliloti	1021
SinmeB_1549	chromosome 1	Sinorhizobium meliloti	BL225C
Arad_2618	chromosome 1	Agrobacterium tumefaciens	K84
Rleg2_1958	chromosome 1	Rhizobium leguminosarum	bv. trifolii WSM2304
Rleg_2169	chromosome 1	Rhizobium leguminosarum	bv. trifolii WSM1325
RL2637	complete	Rhizobium leguminosarum	bv. viciae 3841
RHE_CH02323	chromosome 1	Rhizobium etli	CFN 42
RHECIAT_CH0002420	chromosome 1	Rhizobium etli	CIAT 652
RHECNPAF_426002	unassigned contig	Rhizobium etli	CNPAF512
PDO_1714	unassigned contig	Rhizobium sp. PDO1-076	PDO1-076
Avi_2558	chromosome 1	Agrobacterium vitis	S4
ATU2Av2_I140178	chromosome 1	Agrobacterium genomosp. 2	CFBP 5494
ATU9Av2_I80103	chromosome 1	Agrobacterium genomosp. 9	Hayward 0363
ATU6Av2_I60320	chromosome 1	Agrobacterium genomosp. 6	NCPPB 925
ATU8Av2_I30529	chromosome 1	Agrobacterium fabrum	J-07
AGRO_3558	unassigned contig	Agrobacterium sp. ATCC 31749	ATCC 31749
Atu1874	chromosome 1	Agrobacterium fabrum	C58
ATCR1_18040	unassigned contig	Agrobacterium tumefaciens	CCNWGS0286
ATU4Cv2_I110015	chromosome 1	Agrobacterium tumefaciens	Kerr 14
ATU4Av2_I190150	chromosome 1	Agrobacterium tumefaciens	B6
ATU4Bv2_I60418	chromosome 1	Agrobacterium tumefaciens	CFBP 5621
ATU3Av2_I180009	chromosome 1	Agrobacterium genomosp. 3	CFBP 6623
ATU7Av2_I130082	chromosome 2	Agrobacterium genomosp. 7	NCPPB 1641
ATU7Bv2_I140133	chromosome 1	Agrobacterium genomosp. 7	RV3
ATU7Cv2_I110345	chromosome 1	Agrobacterium genomosp. 7	Zutra 3/1
ATU13v2_I210260	chromosome 1	Agrobacterium genomosp. 13	CFBP 6927
AT5A_15342	unassigned contig	Agrobacterium tumefaciens	5A
ATU1Cv2-I40407	chromosome 1	Agrobacterium genomosp. 1	TT111
AGROH133_07016	chromosome 1	Agrobacterium sp. H13-3	H13-3
ATU1Bv2_I30028	chromosome 1	Agrobacterium ge	
ATU1Av2_I40321	chromosome 1	Agrobacterium tu	
Agau_C200674	chromosome 1	Agrobacterium tu	
ATU5Av2_I10119	chromosome 1	Agrobacterium ge	
MAXJ12_14955	unassigned contig	Mesorhizobium al	
Meso_1263	chromosome 1	Chelativorans sp	
Mesci_4379	chromosome 1	Mesorhizobium ci	
Mesop_4822	chromosome 1	Mesorhizobium op	
MesauDRAFT_4746	unassigned contig	Mesorhizobium au	
MEA186_31136	unassigned contig	Mesorhizobium am	
	chromosome 1	Mesorhizobium lo	

MESSB_2.PE1258 X

Locus Tag	Meso_1267
Length	1214
Description	isocitrate dehydrogenase (NADP)
Reconciled Gene Tree	49RHIZOB_1594